THE ROLE OF PROPROTEIN CONVERTASE SUBTILISIN/KEXIN TYPE 6 IN PLACENTAL DEVELOPMENT UNDER GESTATIONAL DIABETES

A Thesis

by

NAOMI LISA MCCAULEY

Submitted to the Office of Graduate and Professional Studies of
Texas A&M University
in partial fulfillment of the requirements for the degree of

MASTERS OF SCIENCE

Chair of Committee,	Linglin Xie
Committee Members,	Ke (Kurt) Zhang
	Jayanth Ramadoss
Head of Department,	David Threadgill

May 2021

Major Subject: Nutrition

ABSTRACT

Abnormal placenta development has been indicated in preeclampsia and gestational diabetes (GDM), which are both common yet serious complications in approximately 10% of pregnancies. Proprotein convertase subtilisin/kexin-6 (PCSK6) is a protease that processes precursor proteins into active forms. Based on previous reports of PCSK6 expression in the placenta, involvement in embryonic development and vascular remodeling, we hypothesized that PCSK6 plays an important role in placenta development. Our *WT* placentas had a dynamic expression of PCSK6 in glycogen trophoblast cells (GlyT). In mouse hyperglycemic (HG) pregnancies, PCSK6 protein levels were decreased which led us to further pursue the interaction of PCSK6 and HG. The current study applied a PCSK6 transgenic mouse model consisting of four groups: *WT* and *PCSK6 knockout (KO)* placentas from normoglycemic (NG) and HG pregnancies. Histological examination of placenta disclosed that HG, but not *PCSK6 KO*, increased GlyT area within the junctional zone via differentiation. The spiral arteries (SpAs) in *PCSK6 KO* placentas, under NG and HG conditions, had decreased inner to outer diameter ratios and reduced trophoblast giant cell association compared to the *WT* placentas. Consistently, *PCSK6 KO* placentas over-phosphorylate β-catenin, a key protein to regulate transcription of migratory proteins. In the labyrinth, *PCSK6 KO* affected fetal capillary area while HG affected maternal lacunae area. PCSK6 KO-HG placentas had increased interhaemal membrane thickness. From these factors, the calculated diffusion capacity was increased in *PCSK6 KO* under NG but decreased under HG. In summary, our study demonstrated that PCSK6 is involved in SpA remodeling and glucose-dependent angiogenesis. Our study indicated a potential role of PCSK6 in preeclampsia and GDM related placenta dysfunctions. Future study will focus on understanding the molecular mechanisms underlying how PCSK6 deletion disrupted normal placenta development and function.

DEDICATION

To my family and loved ones.

ACKNOWLEDGEMENTS

I would like to thank my committee chair, Dr. Xie, and my committee members, Dr. Zhang and Dr. Ramadoss, for their guidance and support throughout the course of this thesis project and my master's program.

Thanks also go to my friends and colleagues and the department faculty and staff for making my time at Texas A&M University joyous and an opportunity to grow.

Finally, thanks to my mother and father for their encouragement and to my significant other for his patience and love.

CONTRIBUTORS AND FUNDING SOURCES

Contributors

This work was supervised by Professor Linglin Xie and a thesis committee consisting of Professor Linglin Xie, Ke Zhang of the Department of Nutrition and Professor Jayanth Ramadoss of the Department of Veterinary Pathology and Physiology and Pharmacology.

Special appreciation goes towards members of the placenta study group consisting of Yushu Qin, Lauren Lawless, and Zehuan Ding who spent countless hours reading, discussing, and trying out new protocols for our new field of study. Their determination and effort throughout the course of each of our projects were not only essential to the completion of my master's program but also motivated me to give my best. Yushu Qin shared with me some of her WT samples during the beginning of my project. Special thanks also go to Huijuan Zhou, PhD candidate who assisted with several of my statistical methodology throughout the course of my project. I would also like to thank several undergraduate students, Julia Ledbetter, Vanessa Moreno, Anusha Rajbhandari, and Caroline Neal who helped me with my experiments.

All other work conducted for the thesis was completed by the student independently.

Funding Sources

This study is partly supported by grants from the National Institutes of Health (NIDDK 1R01DK112368-01 to Drs. Xie and Zhang) and the USDA National Institute of Food and Agriculture, [Hatch] project [1010406] to Dr. Xie.

NOMENCLATURE

GDM	Gestational diabetes
PCSK6	Proprotein convertase subtilisin/kexin-6
NG	Normal glucose
HG	High glucose / hyperglycemia / hyperglycemic
STZ	Streptozotocin
Lab	Labyrinth
Jz	Junctional zone
Db	Decidua basalis
SynT-I & SynT-II	Syncytiotrophoblast I & II
TGCs	Trophoblast giant cells
S-TGC	Sinusoidal trophoblast giant cells
IHM	Interhaemal membrane
SpT	Spongiotrophoblasts
GlyT	Glycogen trophoblasts
P-TGCs	Parietal trophoblast giant cells
SpA	Spiral artery
EVT	Extra-villous trophoblast
VSMC	Vascular smooth muscle cells
uNK	Uterine natural killer cells
TGFβ1	Transforming growth factor β
TCF/LEF	T-cell factor/lymphoid enhancer factor

MMP	Matrix-metalloproteases
FGF	Fibroblast growth factor
VEGF	Vascular endothelial growth factor
PlGF	Placenta growth factor
PDGF	Platelet-derived growth factor
OR	Odds ratio
sFlt-1	Soluble VEGF receptor -1
ANP	Atrial natriuretic protein
α-SMA	Smooth muscle alpha-actin
SMC	Smooth muscle cells
EL	Endothelial lipase
LPL	Lipoprotein lipase
HE	Hematoxylin and eosin
PAS	Periodic acid-Schiff
RV	Right ventricle
LV	Left ventricle
OFT	Outflow tract
OA	Overriding aorta
AO	Aorta
DORV	Double outlet right ventricle
LD	Lumen diameter
OD	Outer diameter
FCA	Fetal capillary area

MLA	Maternal lacunae area
IGF1	Insulin-like growth factor 1
IGF2	Insulin-like growth factor 2
PRL	Prolactin
Tpbpα	Trophoblast-specific protein α

TABLE OF CONTENTS

LIST OF FIGURES

LIST OF TABLES

Page

CHAPTER I

INTRODUCTION

Background

The placenta grows rapidly by undergoing multiple developmental milestones that establish optimal conditions to support both the offspring and mother during pregnancy. Not only is this organ crucial for a healthy pregnancy, but it also influences the health of both the mother and fetus in their futures. Theories such as "developmental origins of health and disease (DOHaD)" hypothesize that the early life environmental factors affect the risk of developing non-communicable disease later in life through alterations.[1] Therefore, periods of rapid development, such as pregnancy, have been gaining attention from the research community in recent years to find ways to reduce the burden of non-communicable diseases that continue to rise in prevalence.[2] With recognized need for better understanding of the placenta, the National Institute of Health (NIH) initiated and funded over $50 million towards a collaborative research effort called, the "Human Placenta Project (HPP)".[3]

In the 2009-10 National Health and Nutrition Examination Survey (NHANES), it was reported that 55.8% of reproductive age women in the US were either overweight or obese.[4] This is particularly concerning because obesity is a major risk factor for pregnancy complications and can further increase the incidence of gestational diabetes (GDM) and preeclampsia.[5,6] GDM occurs in approximately 7.6% of pregnancies in the United States.[7] Preeclampsia occurs in around 4% of pregnancies in the US.[8] Alarmingly, up to 50% of diabetic pregnancies was reported to develop pregnancy-induced hypertension.[9-11] In addition, clinical history of preeclampsia was reported to increase the risk for developing GDM in subsequent pregnancies.[12]

These statistics on overweight/obese pregnancies, GDM, and preeclampsia are alarming. The fact that they are risk factors of each other indicates a possible commonality in their etiology.

Many pregnancy complications originate from a disruption in placenta development.[13] However, much research is still needed to elucidate their pathophysiology in order to optimize prevention and intervention strategies. In this study, we will investigate the role of proprotein convertase subtilisin/kexin-6 (PCSK6) in placenta development. PCSK6 is a protease that processes precursor proteins into active forms.[14,15] Based on previous reports of PCSK6 expression in the placenta,[16] embryonic development,[17] vascular remodeling,[18] and suppression under HF diet fed pregnancies,[19] we hypothesized PCSK6 to have a role in placenta development particularly under GDM. To investigate the role of PCSK6 under normal glucose (NG) and hyperglycemic (HG) pregnancies, we generated a streptozotocin (STZ)-induced GDM model with *PCSK6 KO* or *PCSK6 WT* placenta. The effect of *PCSK6 KO*, hyperglycemia, and their combined interaction on overall placenta morphology, SpA remodeling, and angiogenesis were assessed. To our knowledge, our study is the first to study the role of PCSK6 within the placenta *in vivo,* and provides new insight into the role of PCSK6 in placenta development.

Placenta developmental milestones

Placenta structure

At glance, the mouse and human placenta have different anatomical structures. The mouse placenta takes on a sponge like, labyrinthine, morphology comprised of trophoblasts with blood perfusion through maternal lacunae or fetal capillaries.[20] On the other hand, the human placenta takes a rather tree-like, villous, structure with the chorionic villi floating in a pool of maternal blood in the intervillous space.[20] On a histology level, the two placentae have similar morphology and functionalities. Both the mice and human placenta are categorized as

hemochorial placentas. In a hemochorial placenta, the maternal blood comes in direct contact with the chorion for humans or trophoblasts for mice.[20]

The mouse placenta contains three layers (from fetal to mothers side): labyrinth (Lab), junctional zone (Jz), and decidua basalis (Db).[21] The mouse Lab is equivalent to the human fetal placenta.[21,22] Different layers of the placenta serve unique functions. The Lab is the site for nutrient, waste, and gas exchange while the Jz serves as a major endocrine site for hormone, growth factors, and cytokine production in the placenta.[21] On a cellular level, the mouse Lab consists of five cell types: fetal endothelial cells, syncytiotrophoblast I & II (SynT-I & SynT-II), sinusoidal trophoblast giant cells (S-TGC), and pericytes.[21,22] The fetal blood is enclosed by fetal capillaries, which is surrounded by trophoblast cells in the order of SynT-II, SynT-I, and S-TGCs (Fig 1). As the placenta matures, the fetal capillaries recruit pericytes.[20,23] The distance between the fetal blood and the maternal blood defined by the layers of trophoblast cells is called the interhaemal membrane (IHM).[21] The thickness of IHM is used as a reference of how efficiently the placenta is able to exchange gas, nutrients, and waste as it represents the distance that these factors need to travel.[21] Between E12.5 and E18.5 of development, serological analysis showed that fetal capillary development occurs in a linear manner while maternal blood space, also called lacunae, expands dramatically between E14.5 and E16.5.[24] Similarly, the IHM undergoes thinning to reach its harmonic thickness by E18.5.[24] The Jz comprises of spongiotrophoblasts (SpT), glycogen trophoblasts (GlyT), and parietal TGCs (P-TGC).[21] The Db consists of mainly maternal cells called decidual cells.[21] These cells were formally endometrial cells that underwent a process called decidualization.[21,25] The Db also contains invasive cells from the pregnancy mass, such as GlyTs and spiral artery (SpA) associated TGCs (SpA-TGCs) (Fig 1). [21,26]

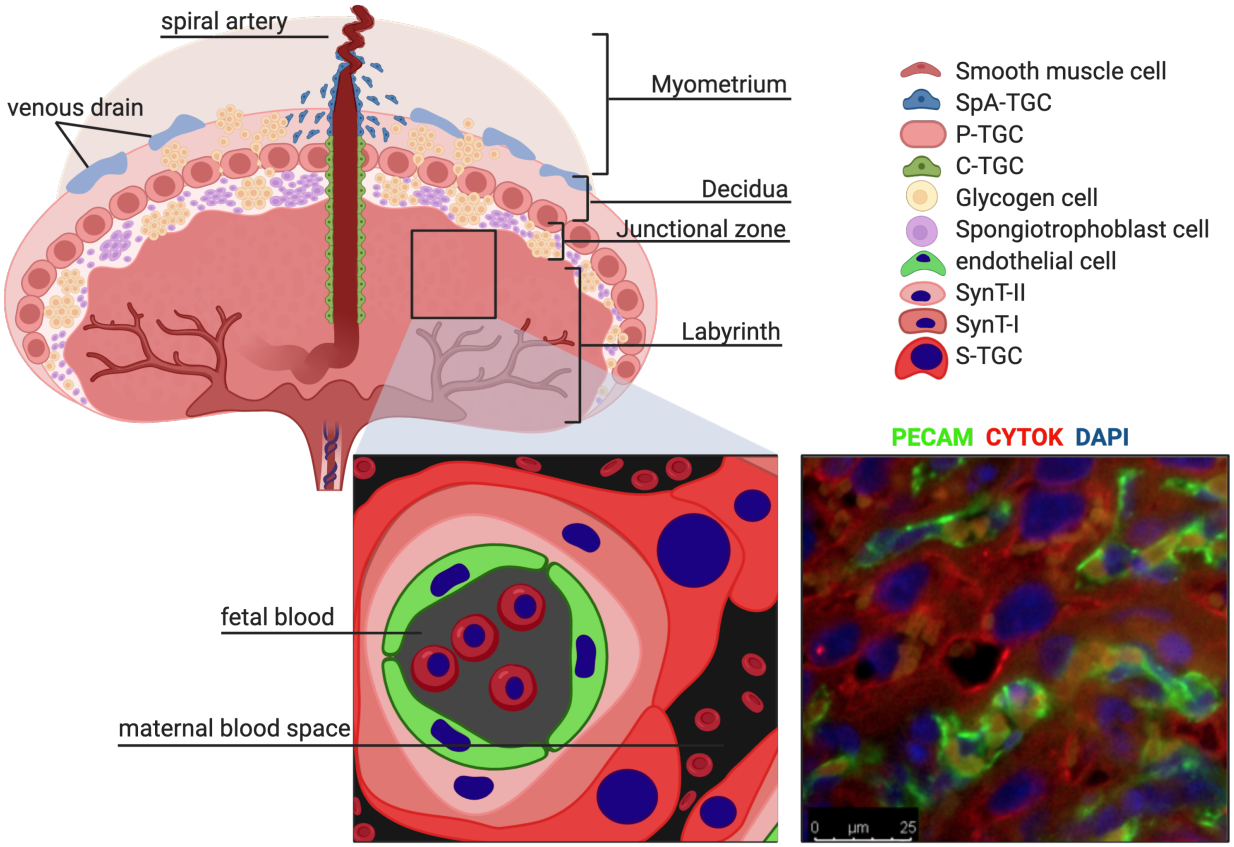

Figure. 1 Structure and cell types of the mouse placenta. Zoomed in box illustrates an abstract diagram of the Lab structure at a cellular level. The histology image to the right is a co-immunofluorescence staining of PECAM and Cytokeratin 18 (Cytok), which stain for the fetal capillaries and placenta trophoblasts, respectively. Cytok stains all trophoblast cells, which include the SynT-I, SynT-II, and S-TGC in the Lab. Created with BioRender.com.

As previously described, the mouse and human placenta appear different in structure but have similar cellular functions in many of their cell types. SynTs also exist in the human placenta where it lines the maternal side of the villi.[27] The SpTs are equivalent to the human column cytotrophoblasts which are stationary and secrete hormones.[27] The P-TGCs are equivalent to the extravillous trophoblasts (EVT).[27] The GlyTs are equivalent to interstitial EVT while SpA-TGCs are equivalent to endovascular EVTs.[27]

Spiral artery remodeling

SpAs in the beginning of the pregnancy are low flow, high resistant arteries surrounded by vascular smooth muscle cells (VSMCs).[28,29] In order to support the needs of the pregnancy mass, these SpA undergo remodeling to become high flow, low resistant arteries.[28,29] SpA remodeling occurs in a stepwise process. First, the uterine natural killer cell (uNK) produces cytokines that cause the VSMCs to undergo apoptosis.[30] These SpAs are then associated/invaded by interstitial and endovascular EVTs (Fig 2).[30] In the human placenta, SpA remoldeing begins in the first few weeks of pregnancy.[30,31] In mouse placenta, TGC migration occurs around E7.5~E10.5.[21]

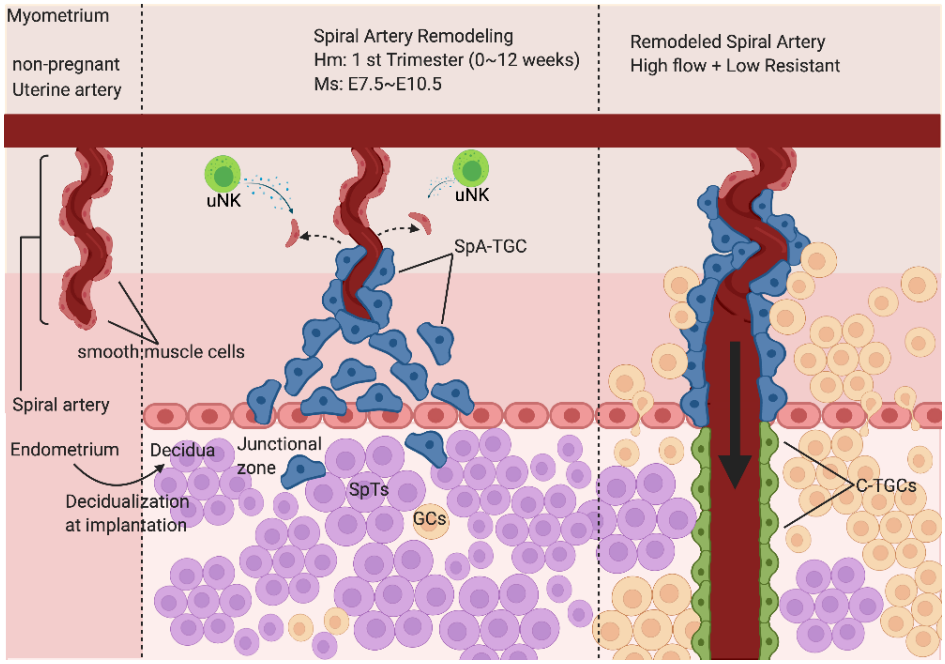

Figure 2. The progression of SpA remodeling in the mouse placenta Db. From left to right, diagrams represent SpA from non-pregnant endometrium, SpA undergoing remodeling, and remodeled SpA. SpA that are yet to be remodeled are high resistant and low flow due to VSMCs organized around the artery (left). Upon conception, the SpAs begin to be remodeled by disorganization of the VSCMs via cytokines secreted by uNKs (middle). The SpA artery then becomes lined with TGCs (middle). These TGCs are then called SpA-associated TGCs (SpA-TGCs). Remodeled SpAs are high flow and low resistant which allows for sufficient flow of blood to the placenta (right). Created with BioRender.com.

Transforming growth factor β1 (TGFβ1) has been described to either promote or inhibit cell migration based on different cell lines.[32-34] However, the popular opinion is that TGFβ1 inhibits trophoblast migration.[35] Additionally, TGFβ1 levels were found to be elevated in the plasma of preeclamptic women.[36]

Wnt signaling has previously been described to be involved in trophoblast migration (Fig 3).[37] The canonical Wnt signaling can be activated by the phosphorylation of GSK3β by Wnt protein ligand or through the PI3K/AKT signaling.[37,38] GSK3β is constitutively active and phosphorylates β-catenin which marks it for degradation by proteasomes.[37,38] GSK3β is deactivated upon phosphorylation and becomes unable to phosphorylate β-catenin.[37,38] GSK3β can be phosphorylated as an effect of Wnt ligand activation or the PI3K/AKT pathway activation.[37-39] This causes the increase in cytoplasmic β-catenin which then also enters the nucleus to form a complex with T-cell factor/lymphoid enhancer factor (TCF/LEF) which increases the expression of genes involved in migration.[37,38] The canonical Wnt signaling has been reported to increase the expression of matrix-metalloproteases (MMP-9) and MT1-MMP.[40,41] MMP-9 and MT1-MMP independently have been found to be expressed in the placenta and invasive cell types.[40,42,43]

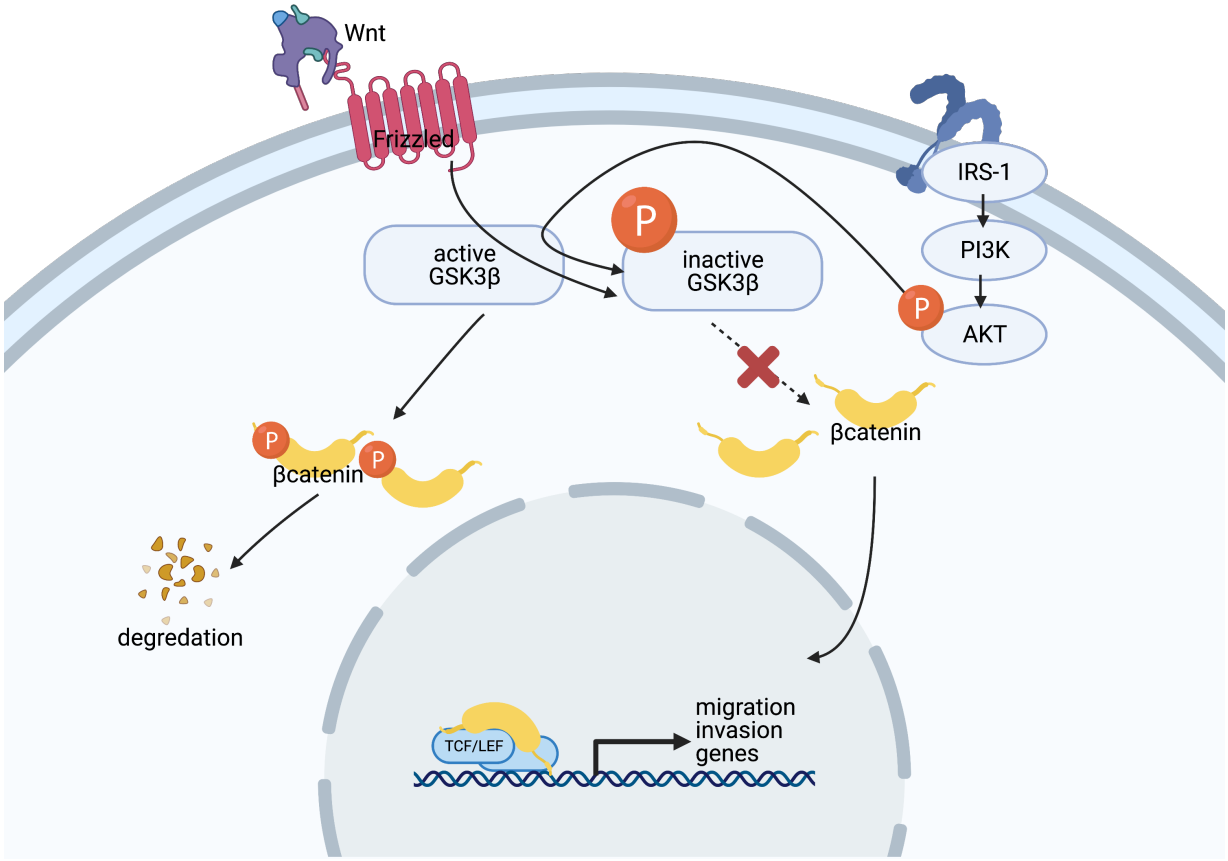

Figure 3. Wnt signaling and trophoblast migration. GSK3β is constitutively active and phosphorylates β-catenin—marking it for degradation. GSK3β is deactivated via phosphorylation—preventing it from phosphorylating β-catenin. This leads to the accumulation of β-catenin levels in the cytosol and nucleus. β-catenin binds with TCF/LEF transcription complex to induce transcription of genes involved in cell migration. GSK3β can be phosphorylated by activated PI3K/AKT signaling or Wnt ligand activation. Created with BioRender.com.

Angiogenesis

The placenta undergoes rapid vascular development to establish the vascular network necessary to accommodate the demands of the developing embryo and fetus. Vascular development originates with vasculogenesis, which is followed by angiogenesis (Fig 4).[44] Vasculogenesis entails the steps from the appearance of hemangiogenic progenitor cells, formation of angioblast cell cords, appearance of first capillaries, and through the development of the primitive capillary network.[44] The vasculogenesis process is usually regulated by growth

factors such as fibroblast growth factor (FGF) and vascular endothelial growth factor (VEGF).[44] Later, angiogenesis takes over and causes sprouting and branching of the capillary network.[44] The angiogenesis process is regulated by the VEGF and placental growth factor (PlGF).[44] In the human placenta, vasculogensis occurs in the 1st trimester while the angiogenesis process occurs in the 2nd trimester.[44] In the mouse placenta, the villi vascularization occurs early as E8.5 to E10.5 which is equivalent to the 1st trimester of the human pregnancy.[31] At E13.5, increased levels of platelet-derived growth factor β (PDGFβ) is suggested to regulate the development of labyrinth by modulating pericyte growth.[45]

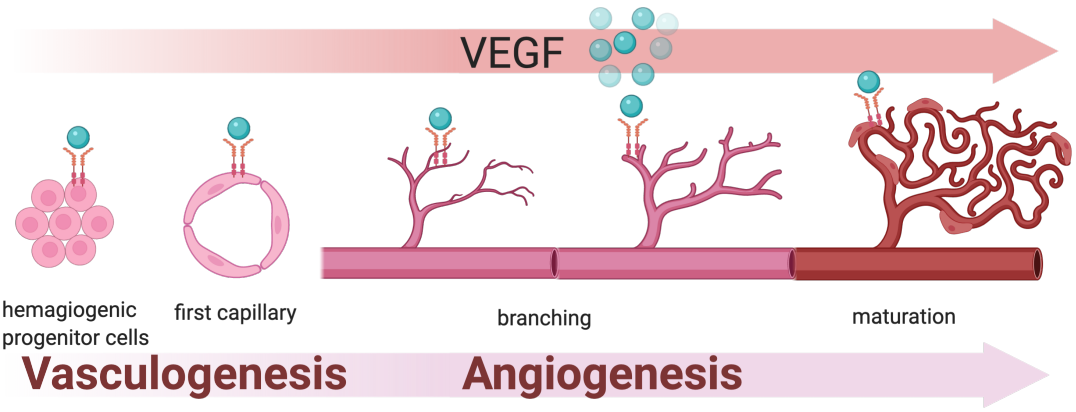

Figure 4. The progression of angiogenesis in the mouse placenta Lab. The Lab undergoes vasculogenesis which forms the first capillaries. Then angiogenesis takes over to further increase the branches of the fetal capillaries. Fetal capillaries then recruit the development of pericytes. Created with BioRender.com.

Placental origins of pregnancy complications

Pregnancy complications such as GDM and preeclampsia originate from perturbations in various developmental processes.[13] Many studies have reported risk factors and observed pathophysiology of these diseases,[13] but much of the molecular etiology still remains unclear.

GDM and placenta

Increased placental leptin production and pro-inflammatory cytokines have been suggested to cause insulin resistance in GDM.[46] Other molecular processes that have been hypothesized to contribute to GDM include, β-cell dysfunction, chronic insulin resistance, and gut dysbiosis.[46] Clinically, placentas from GDM women have been associated with villous immaturity, chorangiosis, and increased angiogenesis.[47] Although the precise mechanisms are yet to be fully elucidated, these abnormal-excessive vascular developments have been described to develop in response to chronic low grade hypoxia.[48,49] Increased angiogenesis has been associated with decreased VEGFR1 and increased VEGFR2 mRNA levels with no change in VEGFA mRNA.[50] These results suggest that GDM etiology involves the placenta, but GDM itself can also alter placenta vascular development.

Preeclampsia and placenta

Defects in the process of SpA remodeling is commonly described to be the cause of complications such as early-onset preeclampsia and fetal growth restriction (FGR).[51] It is suggested that the abnormal trophoblast invasion and SpA remodeling leads to placental hypoxia which, in turn, increases inflammatory factors to be produced by the placenta.[51,52] These changes result in endothelial dysfunction that leads to increased reactive oxygen species and decreased nitric oxide production.[51,53] Ultimately, this leads to increased maternal total peripheral resistance and decreased glomerular filtration rate.[51,53] These physiological changes in the mother result in hypertension.[51-53] With high maternal and perinatal morbidity and mortality, preeclampsia is considered one of the most dangerous pregnancy complications.[54]

Common etiology of preeclampsia and GDM

Alarmingly, up to 50% of diabetic pregnancies were reported to develop pregnancy induced hypertension.[9-11] In the US, patients with severe or mild preeclampsia are about 1.5 times likely to have had GDM.[55] Increased soluble VEGF receptor -1 (sFlt-1) concentrations in the serum have been reported to predict the risk for developing preeclampsia.[56] Similarly, GDM placenta have been reported to have increased sFlt-1 levels compared to normal pregnancies.[57] Indeed, mid-trimester maternal insulin resistance has been reported to be associated with subsequent preeclampsia risk.[58] However, a more detailed picture of preeclampsia and GDM, individually and in relation to each other, is yet to be mapped. We hope our study contributes to unveil some of these unknown gaps in etiology.

Proprotein convertase subtilisin kexin type 6

General functionality

The enzyme PCSK6 belongs to the subtilisin-like proprotein convertases (PCs) family. PCSK6 is a Ca^{2+} dependent serine protease and cleaves a number of proproteins with a general sequence of (K/R)-(X)n-(K/R)↓.[14,15] In this motif, n can be 0,2,4, or 6 while X being an amino acid that is not Cys.[15] In literature, PCSK6 can also be called as subtilisin-like proprotein convertase 4 (SPC4), or paired basic amino acid cleaving enzyme 4 (PACE4).[59,60] Pro-PCSK6, which could be a monomer or dimer, undergoes an autocatalytic process in the ER to be released as a mature monomer form of PCSK6 which localizes extracellularly.[59,60] In the ECM, PCSK6 was found to bind heparin, which indicates an interaction with heparan sulfate proteoglycans.[61] Proteoglycans are spatially-and-temporally expressed and enhance receptor signaling by binding ligands in the ECM.[61-64] Similar to PCSK6, MMPs have also been suggested to associate with proteoglycans.[65] The binding of heparin with PCSK6 and developmental factors suggests that

PCSK6 is likely to be involved in regulating signaling molecules which require strict spatiotemporal regulation, such as those in the placenta.[61]

PCSK6 expression in the human body

According to the human protein atlas data base available to the public, PCSK6 levels does show some heterogeneity in expression levels.[16] On a tissue mRNA level, *PCSK6* is highly expressed in the brain, liver, lymphoid tissues, and the placenta (Fig 5A).[16] On a single cell level, *PCSK6* is highly expressed in hepatocytes and horizontal cells (Fig 5B).[16] To note, EVTs came in third for cell types expressing high levels of *PCSK6* (Fig 5B).[16] In the blood, the NK cells express the highest *PCSK6* RNA levels (Fig 5C).[16] From all of these data sets, it can be suggested that PCSK6 has a role in development of placenta, as well as NK cells known to be involved in SpA remodeling.

A

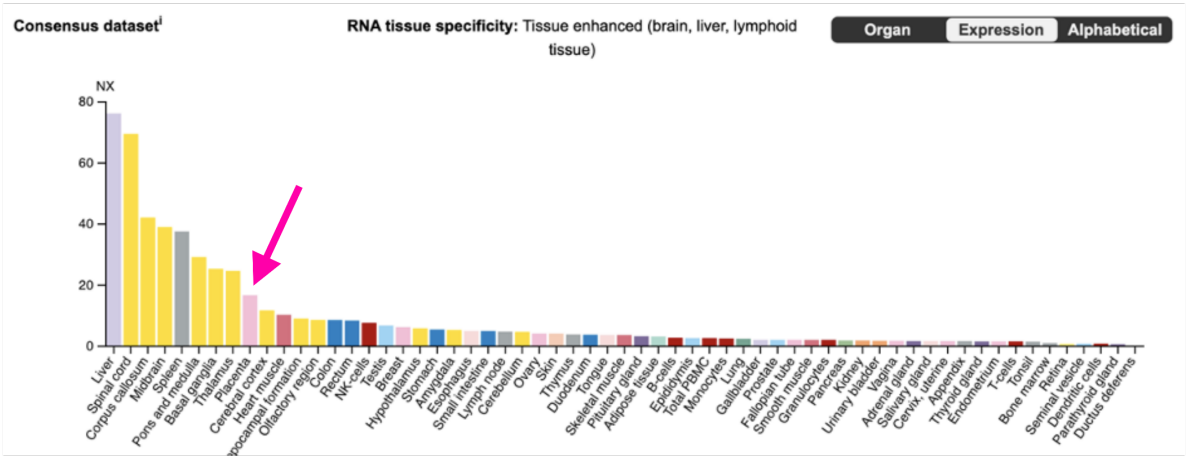

B

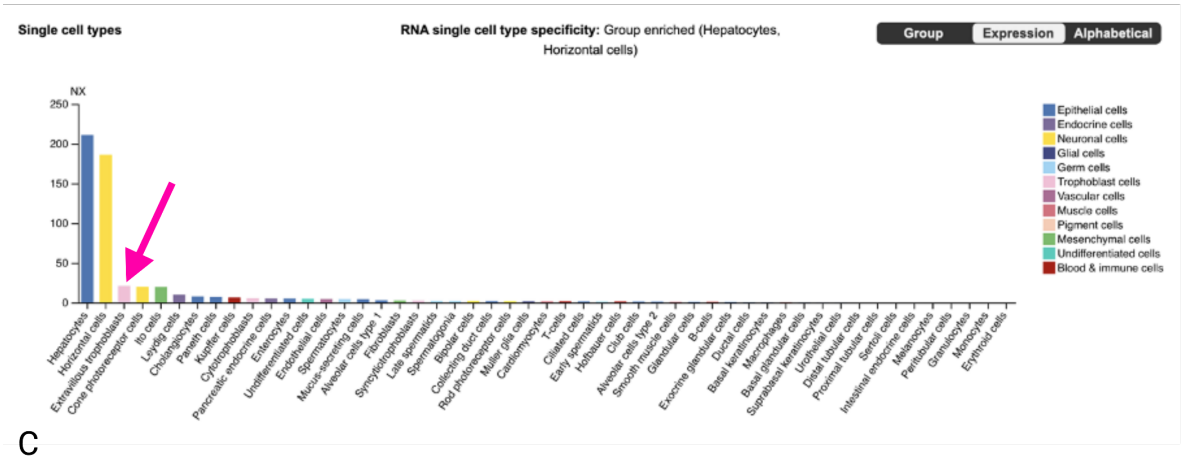

C

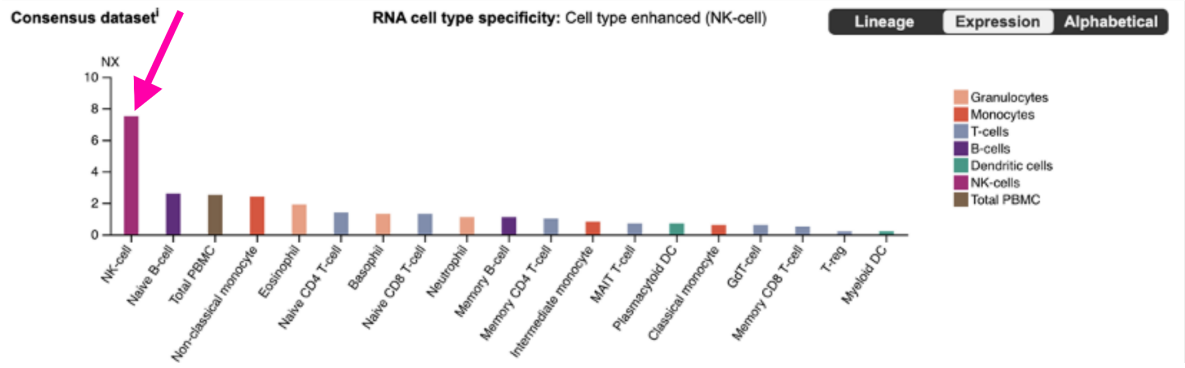

Figure 5. PCSK6 expression data from the Human Protein Atlas. (A-C) PCSK6 mRNA in different tissues, single-cell, and cells in the blood, respectively. Pink arrows are added to indicate the placenta-related tissue and cell types mentioned in the text. (A) Image/gene/data available from v20.proteinatlas.org/ENSG00000140479-PCSK6/tissue. (B) Image/gene/data available from v20.proteinatlas.org/ENSG00000140479-PCSK6/celltype. (C) Image/gene/data available from v20.proteinatlas.org/ENSG00000140479-PCSK6/blood. Figure 5 itself compiled images from Human Protein Atlas using BioRender.com.

PCSK6 in cancer

PCSK6 has been associated with several invasive cancer types.[66-68] In breast cancer MDA-MB-231 cells, PCSK6 was found to reduce cell cycle arrest by activating extracellular signal-regulated kinase1/2 and Wnt3A pathways.[66] In human prostate cancer, PCSK6 has been found to be overexpressed, and its targeted silencing in DU145 prostate cancer cell lines decreased their proliferation and xenographic abilities.[67] In murine skin keratinocytes, overexpression of PCSK6 resulted in its conversion to malignant cells that had enhanced processing for MMP-11 and MT2-MMP which processes MMP-2 and MMP-9, well known migratory proteins.[68]

PCSK6 in development

Previous studies on PCSK6 identified many of its functions in cleaving developmental regulators. When PCSK6 was overexpressed, Nodal and BMP4 processing increased.[69] In a germline *PCSK6 KO* mouse model, in which PCSK6 cleavage site is made non-functional, the embryos developed situs ambiguous, left pulmonary isomerism, and craniofacial defects.[17] A whole mount in situ hybridization showed that *PCSK6* is expressed in the foregut, and is crucial for A/P axis formation, such as the anterior CNS development.[17] *PCSK6 KO* mice had increased rates of embryonic failure, which were associated with major issues in heart development, evidenced by instances of double outlet right ventricle, persistent truncus arteriosus, single chamber, septum defects, and dextrocardia.[17] Gene expression analysis of early somite showed that Nodal, Pitx2, Lefty1 and Lefty2 are genetically downstream of PCSK6 indicating involvement of PCSK6 in regulating Nodal and BMP signaling important for the L/R axis formation.[17] From these studies that looked into PCSK6 in early development, PCSK6 is suggested to play a role in early patterning.

PCSK6 in reproductive organs

PCSK6 was found to be highly expressed in granulosa cells of pre-ovulatory follicles.[70] Here, PCSK6 levels were up-regulated upon stimulation by luteinizing hormone.[70] On the other hand, when PCSK6 was disrupted, apoptosis was promoted in conjunction with increased activin A and TGFβ2 levels and decreased follastin levels.[70] In mice with non-functional PCSK6 (PCSK6tm1Rob), progressive loss of ovarian function and alterations in expression of genes involved in steroidogenesis, gonadotropin signaling, and cholesterol handling was reported.[71] These reports indicate that PCSK6 plays a role in normal cellular homeostasis of reproductive organs. Alarmingly, PCSK6 levels can be altered by metabolic status. This was evidenced in a decreased PCSK6 levels in hyperinsulinemic rat model fed a HF diet.[19]

PCSK6 in vascular regulation

In recent years, PCSK6 has been gaining attention in the field of cardiovascular diseases. Surprisingly, PCSK6 was found to be involved in blood pressure regulation when PCSK6 KO mice developed salt sensitive hypertension.[72] Chen et al found that PCSK6 cleaves the precursor of corin, which is upstream of atrial natriuretic protein (ANP).[72] Interestingly, corin and ANP independently were also found to be essential for SpA remodeling.[73] When corin or ANP was knocked-out, mice exhibited preeclamptic symptoms and issues with SpA remodeling evidenced by smaller SpA diameter and less trophoblast association with SpAs.[73]

PCSK6 was also found to be associated with atherosclerosis when its expression was found to be high in the fibrous caps of symptomatic carotid plaques.[74] In these symptomatic plaques, PCSK6 proteins were localized in smooth muscle alpha-actin (α-SMA) positive cells, extracellular matrix of the fibrous cap, and neovessels.[74,75] Later, PCSK6 was found to be a key enzyme for controlling smooth muscle cell migration in vascular remodeling.[75] Upon stimulation

with PDGFβ, PCSK6 levels increased.[75] Five days after the injury of a rat carotid artery, PCSK6 and MMP14 were found to co-interact in smooth muscle cells (SMCs).[75] At two weeks after the injury, PCSK6 was found to be co-expressed with both MMP14 and MMP2.[75] MMP14, also known as MT1-MMP, is a matric metalloproteinases (MT-MMP) that was discovered as an activator of pro-MMP2.[76-78] MT1-MMP has since been described in cell invasion/migration[42,75,79], proliferation,[80] and angiogenesis.[81] Consistently, when PCSK6 was knocked out, MMP14 levels decreased and showed decrease in smooth muscle cell migration.[75]

PCSK6 in lipid metabolism

PCSK6 has been described to process endothelial lipase (EL) and lipoprotein lipase (LPL) which makes PCSK6 a regulator of HDL metabolism.[82,83] The inactivation of EL and LPL by proteolytic cleavage affects HDL cholesterol concentration.[82] Although PCSK3, PCSK5, and PCSK6 are all able to cleave EL and LPL, PCSK6 is most efficient in cleaving EL.[83]

Scientific question and hypothesis

From literature, PCSK6 is suggested to be involved in various physiological processes by processing different enzymes. With high levels of PCSK6 reported to be expressed in the placenta,[16] we hypothesize that PCSK6 has a role in placenta development. In our study, we will investigate the role of PCSK6 in placenta development by identifying its spatial and temporal expression in the placenta. We will utilize a *PCSK6 KO* mouse model to investigate the phenotypes and growth markers of placentas void of functional PCSK6. From this exploratory effort, we aim to identify specific developmental processes that PCSK6 is involved in.

PCSK6 was also reported to have a lower expression in the placenta of HF-diet fed hyper-insulinemic rats.[19] This suggests to us that the levels and function of PCSK6 in the placenta is altered under adverse nutritional and/or metabolic status of the mother. Therefore, in

this project, we will investigate the effects of hyperglycemia on the profile of PCSK6 and overall development of the placenta.

With our study design, we are able to look into the important role of PCSK6 in placenta development under normoglycemia and hyperglycemia, which further elucidates the interactive role of PCSK6 deletion and hyperglycemia on placenta development. Through our findings, we hope to expand the understanding of placenta development, which could ultimately lead to better nutritional and medical therapeutic practices for preventing and treating pregnancy complications, including GDM and preeclampsia.

CHAPTER II

EXPERIMENTAL METHODS

Experimental design-mouse

We utilized a *PCSK6 KO* transgenic mouse model to study how *PCSK6 KO* would affect placenta development. Germline *PCSK6 KO* mice were generously gifted by Dr. Anne-Marie Malfait, Department of Internal Medicine (Rheumatology), Rush University Medical Center, Chicago, Illinois. These *PCSK6 KO* mice had a vector-deletion that spanned its catalytic serine which made the translated PCSK6 protein non-functional as previously described.[17] *PCSK6 KO* mice were backcrossed with C57BL/6 background mice. In order to generate placenta with and without functional PCSK6 protein, we crossed germline *PCSK6*$^{+/-}$ male breeders with either *PCSK6 WT* or *PCSK6 KO* female dams. From these crosses, we generated four placentas with varying genotypes (maternal genotype | embryo genotype): *WT* | *WT*, *WT* | +/-, *KO* | +/-, and *KO* | *KO* (Figure). For abbreviation purposes, *WT* | *WT* placenta will be termed as WT, and *KO* | *KO* placenta as KO.

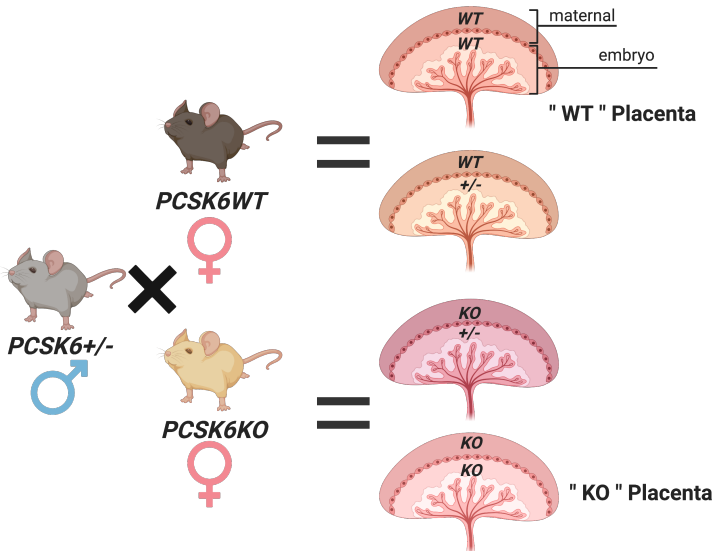

Figure 6. Mouse breeding plan and possible placenta genotypes. Placentas with both the maternal and fetal side of the genotype consisting of *PCSK6*+/+ is referred to as WT placenta. Placentas with both the maternal and fetal side of the genotype consisting of *PCSK6*-/- is referred to as KO placenta. Created with BioRender.com.

Experimental design-STZ induced GDM

In addition to the genetic variation, we also separated the dams into either euglycemia or hyperglycemia groups to investigate the effects of *in utero* hyperglycemia on placenta and embryo development. Hyperglycemia was induced using STZ intraperitoneal injections at 100 mg per kg body weight dissolved in sodium citrate (SC). STZ is cytotoxic to pancreatic β cells, therefore, induces hyperglycemia by decreasing insulin secretion.[84] STZ treatments were given twice with two days in between. On the second day of injections, the female mice were bread with the *PCSK6+/-* breeders overnight. At separation, the mice were considered E0.5. Blood glucose and body weight were measured on each day of STZ injection, E3.5, E7.5 and E14.5 at which time the placentas were collected and micro-dissected. The schematic timeline of treatment and major developmental milestones are illustrated in Figure 7.

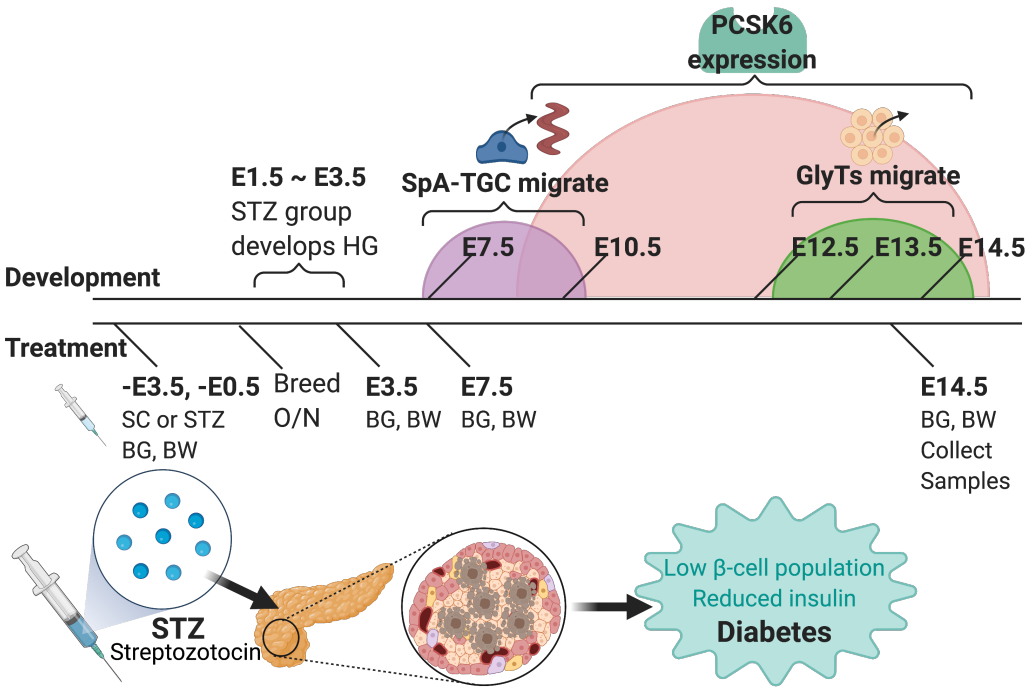

Figure 7. Major developmental timeline (top) overlapped with treatment timeline (bottom). The timeline for STZ treatment, major placenta development, and PCSK6 expression in the whole placenta are overlapped. Created with BioRender.com.

Experimental design-treatment groups

With the breeding and treatment plan, eight possible groups were generated (Table 1). In this thesis, analysis was done on four groups: WTNG, KONG, WTHG, and KOHG. We compared amongst these four groups to investigate the effects of *PCSK6 KO* and/or hyperglycemic pregnancies. Mouse experiments were conducted according to a protocol reviewed and approved by the Institutional Animal Care and Use Committee of Texas A&M University. Our protocol is in compliance with the USA Public Health Service Policy on Humane Care and Use of Laboratory Animals.

Table 1. Summary of all sample groups generated from genetic and glucose conditions.

Breeder genotype	Dams genotype	Treatment	Fetal genotype	Placenta Group
$PCSK6^{+/-}$	$PCSK6^{WT}$	NG	$PCSK6^{WT}$	$PCSK6^{WT\|WT}$|NG
			$PCSK6^{+/-}$	$PCSK6^{WT\|+/-}$|NG
$PCSK6^{+/-}$	$PCSK6^{KO}$	NG	$PCSK6^{+/-}$	$PCSK6^{KO\|+/-}$|NG
			$PCSK6^{-/-}$	$PCSK6^{KO\|KO}$|NG
$PCSK6^{+/-}$	$PCSK6^{WT}$	HG	$PCSK6^{WT}$	$PCSK6^{WT\|WT}$|HG
			$PCSK6^{+/-}$	$PCSK6^{WT\|+/-}$|HG
$PCSK6^{+/-}$	$PCSK6^{KO}$	HG	$PCSK6^{+/-}$	$PCSK6^{KO\|+/-}$|HG
			$PCSK6^{-/-}$	$PCSK6^{KO\|KO}$|HG

Human placenta sample

Paraffin slides of full-term placenta of normal or patients diagnosed with gestational diabetes (n=10) were obtained from Dr. Lanjing Zhang (Princeton Medical Center and Rutgers University). The slides were used to assess the expression of PCSK6 in placenta.

Placenta collection

Placenta samples were collected at E14.5 and micro-dissected into two sagittal halves: one side for molecular experiments and the other half for histology purposes. As described in the introduction section, the mouse placenta has layers known for different developmental processes, gradients and distribution of growth factors and receptors. To this extent, when analyzing different developmental processes on a molecular level, the placentas were micro-dissected into two main layers: Lab and Jz+Db.

Histology

Different histology techniques were used to investigate the effect of *PCSK6 KO* and/or hyperglycemia on overall placenta morphology, SpA remodeling, and angiogenesis processes.

Tissue processing, embedding, sectioning, and deparaffinization

The collected placentas were fixed in formalin for two days, stored in 70% EtOH, and then processed in an automated tissue processor with the following program:

For E10.5 placenta:

70% EtOH (20 mins), 80% EtOH (10 mins), 95% EtOH-1 (10 mins), 95% EtOH -2(8 mins), 100% EtOH-1 (5 mins), 100% EtOH-2 (5 mins), 100% EtOH-3 (6 mins), xylene-1 (8 mins), xylene -2(7 mins), xylene-3 (15 mins), paraffin-1 (30 mins), and paraffin-2 (40 mins).

For E12.5, E14.5, and E16.5 placenta:

70% EtOH (50 mins), 80% EtOH (25 mins), 95% EtOH-1 (25 mins), 95% EtOH-2 (25 mins), 100% EtOH-1 (10 mins), 100% EtOH-2 (10 mins), 100%EtOH-3 (20 mins), xylene-1 (10 mins), xylene-2 (15 mins), xylene-3 (25 mins), paraffin-1 (40 mins), and paraffin-2 (120 mins).

After tissue processing, the placentas were then embedded in paraffin, and stored at room temperature until sectioned. The sectioning of the placenta was done in 5 μm sagittal cuts. Sectioned placenta slides were deparaffinized by incubating at 60 °C for 30 mins, xylene-1(10 mins), xylene-2 (10 mins), 100% Flex-1 (1 min), 100% Flex-2 (1 mins), 95% Flex-1 (1 min), 80% Flex, 50% Flex (1 min), washed under running tap water (5 mins), and then underwent chemical staining or antigen retrieval for immune-staining.

Hematoxylin & eosin staining

One of the assessments we did on SpA remodeling was measuring the length of the shorter diameter of the inner and outer lumens of the SpA in the distal portion of the Db. Hematoxylin and eosin (HE) staining were used to visualize the stroma of the SpAs. Deparaffinized slides were then placed in hematoxylin (1.5 mins), running tap (3 mins), 1% acidic alcohol solution (dip), running tap (2 mins), 1% ammonium hydroxide (1 min), 70% EtOH (2 min), Eosin-Y (1 min), and running tap (1 min). The stained slides were then placed in a 60 °C oven for 20 mins, cooled to room temperature, and then mounted with paramount.

Periodic acid-Schiff staining

Glycogen granules were stained with Periodic acid-Schiff (PAS) staining which allows for differentiation of the Jz from the Lab and Db, and GlyTs from the SpTs within the Jz. Deparaffinized slides were incubated in periodic acid solution (5 mins, Sigma-Aldrich catalog No. 3951, 1g /dL) at room temperature, dH_2O (3 times, 2 mins each), Schiff's reagent (15 mins, Sigma-Aldrich catalog No.3952), running tap (5 mins), counterstain with hematoxylin (1.5 mins), running tap (5 mins), dipped in Scott's tap water (1L dH_2O, 2g $NaHCO_3$, 20g $MgSO_4*7H_2O$), and running tap (1 min). The stained slides were then placed in a 60 °C oven for 20 mins, cooled to room temperature, and then mounted with paramount. PAS-stained slides

were scanned at 400x using Aperio Slide Scanner and analyzed using ImageScope. Using the free-hand tracing tool, the whole placenta (excluding the myometrium), Jz, and Lab were traced. Within the Jz, the space and GlyT areas were traced. SpT area was calculated as follows:

$$SpT\ area = Jz - Space - GlyT$$

Sirius red staining

Placentas were stained with Sirius red to investigate for fibrosis, a common pathological feature of preeclamptic placentas.[85] The deparaffinized placentas were incubated with Sirius red solution (60 mins, ab150681). Then, the slides were dipped in 2 changes of 0.5% acetic acid solution (diluted from Sigma-Aldrich 338826) and 3 changes in absolute alcohol. The stained slides were then placed in a 60 °C oven for 20 mins, cooled to room temperature, and then mounted with paramount.

Antigen-retrieval and immunostaining

For antigen retrieval, deparaffinized slides were placed in 50 mL of dH_2O coplin jar with 500 µL of concentrated antigen retrieval buffer and steamed (20 mins), cooled (10 mins), and rinsed in running tap (5 mins).

For immunofluorescent staining, slides were incubated in TrueBlack (Fisher catalog No.NC1125051) to reduce unspecific staining and blocked in 2% goat serum (30 mins), and then incubated with 1° antibody diluted with 2% goat serum for 18 hours. The slides were then washed with PBS (2 times, 3 mins each) and incubated with 2° antibody diluted with 2% goat serum for 30 mins. The slides were washed again with PBS (2 changes, 3 mins each) and then mounted with Flo Dapi.

For immunohistochemistry, deparaffinized slides were incubated in 3% H_2O_2 (10 mins) and PBS (3 times, 2 mins each), blocked in 2% goat serum (30 mins), and then incubated with 1°

antibody diluted with 2% goat serum for 18 hours. The slides were rinsed with PBS (2 changes, 3 mins), biotinylated secondary antibody (30 mins, VECTASTAIN® ABC-HRP Kit, Peroxidase (Rabbit IgG) PK-4001), ABC (30 mins, VECTASTAIN® ABC-HRP Kit, Peroxidase (Rabbit IgG) PK-4001), DAB (until color develops, ImmPACT® DAB Substrate, Peroxidase (HRP) SK-4105)), and counterstained with hematoxylin (10 secs, Hematoxylin QS Counterstain H-3404). The slides were rinsed under running tap for 5 mins and then placed in a 60 °C oven for 20 mins, cooled to room temperature, and then mounted with paramount. The following antibodies were used (Table 2).

Table 2. Antibodies used for histology.

Type	1° Antibody	Analysis	Purpose
IHC	PCSK6 (ab140934)	Identify cells with + staining	PCSK6 profile
IF	Tpbpα (ab104401)	Count cells with Tpbpα+ staining	GlyT cell count
IF	p-H3S10 (ab5176)	Count cell pH3S10+ cells	Proliferation
Co-IF	Cytokeratin 18 (ab668): SpA-TGCs, PECAM (Cell77699): endothelial cells	Degree of Cytok+ TGCs present on SpAs in distal Db	SpA remodeling
Co-IF	PECAM (Cell77699): endothelial cells Cytokeratin 18 (ab668): SynT-I, SynT-II, sTGCs	Measure fetal and maternal blood space Measure distance from fetal to maternal blood space	Degree of vascularity Thickness of IHM
Co-IF	PECAM (Cell77699): endothelial cells α-SMA (ab7817): pericytes	Count a-SMA+ profiles	Degree of vascular maturity
IF or Co-IF: 2° Antibody		Host of 1° Antibody	
Alexa Flour 488 goat anti-rabbit (A11008)		Rabbit	
Alexa Flour R 594 donkey anti-mouse (A21203)		Mouse	
Alexa Flour 594 goat anti-rat (A11007)		Rat	

Analysis of SpA-TGC association with SpAs

The association of TGCs with SpAs in the distal Db was measured using a co-IF staining of PECAM and Cytok (Table 2). Identified SpAs in the distal portion of the Db were classified into three categories based on Cytok lining: fully associated (over 75%), partially associated (25~50%), and non-associated (less than 25%). If more than 50% of its SpAs were either partially or fully associated with TGCs, a placenta sample was counted as a "TGC-associated" sample. If less than 50% of it was either partially or fully associated, then the sample was counted as an "not associated" sample. Based on this per placenta sample categorization, simple linear regression and Chi-Square tests were performed.

Analysis of fetal and maternal blood space

The fetal and maternal blood space area were measured using PECAM and Cytok similarly to what has previously been performed (Table 2).[86] Images were taken at 200x. With PECAM staining for fetal endothelial cells, we traced the outer lining of fetal capillaries defined by PECAM+ staining. Cytok stains for all trophoblast cells in the Lab. Therefore, maternal lacunae area (MLA) was defined by spaces not stained by PECAM, Dapi, nor Cytok. Due to the skewed nature of the sizes of area measurements, the total sum of the log transformed values of all fetal capillary area (FCA) selections was calculated for each placenta to be used for statistical analysis. The same was done for MLA. The surface area (=mean of total FCA and total MLA) were calculated for each sample. We used ImageJ for analyzing the images.

Analysis of IHM thickness

The IHM thickness is the distance between fetal and maternal blood space. Using the Co-IF staining of PECAM and Cytok imaged at 200x, 20 locations of IHM were measured using ImageJ. IHM thickness and the mean surface areas of the fetal capillary area and maternal

lacunae area allowed for the estimating of theoretical diffusion capacity of the Lab using the following equation:

$$D = K * (\frac{mean\ surface\ area}{IHMthickness})$$

In the aforementioned equation, D stands for diffusion capacity, and K stands for Krough diffusion coefficient for oxygen (17.3×10^{-8} cm^2 min^{-1} kPa^{-1}). This equation was described in a paper that analyzed the morphometric diffusing capacity using mean surface area and IHM thickness obtained from different methods.[24] However, as the measurements should theoretically represent the same thing, the above equation was used.

Analysis of pericyte development

Pericyte development was measured to assess the maturation of the Lab angiogenesis. The pericytes were stained using α-SMA (Table 2). The number of pericytes profiles over counted area was measured using ImageJ.

Molecular Assays

Western blot

Proteins were extracted from either the whole placenta or the separated layers of Lab or Jz+Db. Once boiled with SDS, each well was loaded with 20 ng of protein. Proteins were transferred to membranes and blocked for 2 hours in 5% milk in TBST. Membranes were incubated overnight with 1° antibody overnight (18 hours) (Table 3).

Table 3. Antibodies used for WB.

1° Antibody	Concentration	Tested layer	Analysis	Purpose
PCSK6 (ab140934)	1:1000	Whole, Lab, Jz+Dz	Identify change in Pcsk6 overtime and under HG	PCSK6 profile
Phospho-β-catenin (ab9561)	1:1000	Jz+Dz	Wnt siganling	SpA remodeling
β-catenin (CellSig8480)	1:1000	Jz+Dz	Wnt signaling	SpA remodeling
TGF-β1 (CellSig3709)	1:1000	Jz+Dz	TGF-β signaling	SpA remodeling
Vinculin (CellSig13901)	1:1000	Jz+Dz	Housekeeping	Loading control
Gapdh (CellSig2118)	1:5000	Lab, Jz+Dz	Housekeeping	Loading control
2° Antibody	Concentration			
Anti-Ms IgG HRP-linked Antibody (CellSig 7076)	1:3000			
Anti-Rb IgG HRP-linked Antibody (CellSig7064)	1:3000			

Statistical analysis

All statistical analyses and graph generations were performed on GraphPad Prism version 9 for macOS. Treatment effects such as hyperglycemia, *PCSK6 KO*, and their interaction were assessed via two-way ANOVA or simple logistic regression. Based on the two-way ANOVA results, follow-up Fisher LSD results are shown on the graphs. Simple logistic regression's likelihood test was followed up with $\chi 2$ test. P-values are noted as *($p<0.05$), **($p<0.01$), ***($p<0.001$), ****($p<0.0001$). Number of samples (embryos, placentas) used for the study are noted as n = (x). The numbers of pregnancies the samples were sampled from are noted as m = (x).

CHAPTER III

RESULTS

PCSK6 expression in mouse placenta and human placenta under NG

Expression of PCSK6 in mouse and human placentas was visualized by IHC staining (Fig 8). In the E14.5 Ms placenta, PCSK6 was identified mostly in the Jz and Db area specifically in the GlyTs (Fig 8A). There were few clusters of PCSK6 expressing cells in the Lab, but these were mostly ectopic GlyT clusters (Fig 8A). In the term human placenta, PCSK6 was identified in the SynT toward the basal plate, mesenchymal stromal cells, and stromal and decidual cells of the basal plate (Fig 8B).

When PCSK6 was stained in mouse placentas collected over time, we observed a shift in location. Originally, PCSK6 expression was very low and started near the ectopic cone (Fig 8C). Then by E12.5, PCSK6 expression increased in the GlyTs of the developing Jz (Fig 8C). By E14.5, PCSK6 expressing GlyTs had begun to migrate towards the Db (Fig 8C). When expression levels of PCSK6 in whole placenta lysates were detected, PCSK6 had a transient expression between E10.5 and E16.5 with the highest at E12.5 (Fig 8D, E). The PCSK6 expression with IHC shows that the expression of PCSK6 along with the GlyT population appears to increase over time. This is not consistent with the PCSK6 protein levels from the whole placenta lysate showing a peak at E12.5. This discrepancy may be due to the western blot using the whole placenta lysate which would not reflect the PCSK6 protein levels localized in the Jz and Db. Nevertheless, on a histology level, the IHC staining of PCSK6 shows a high expression which persists from E14.5 and into E16.5.

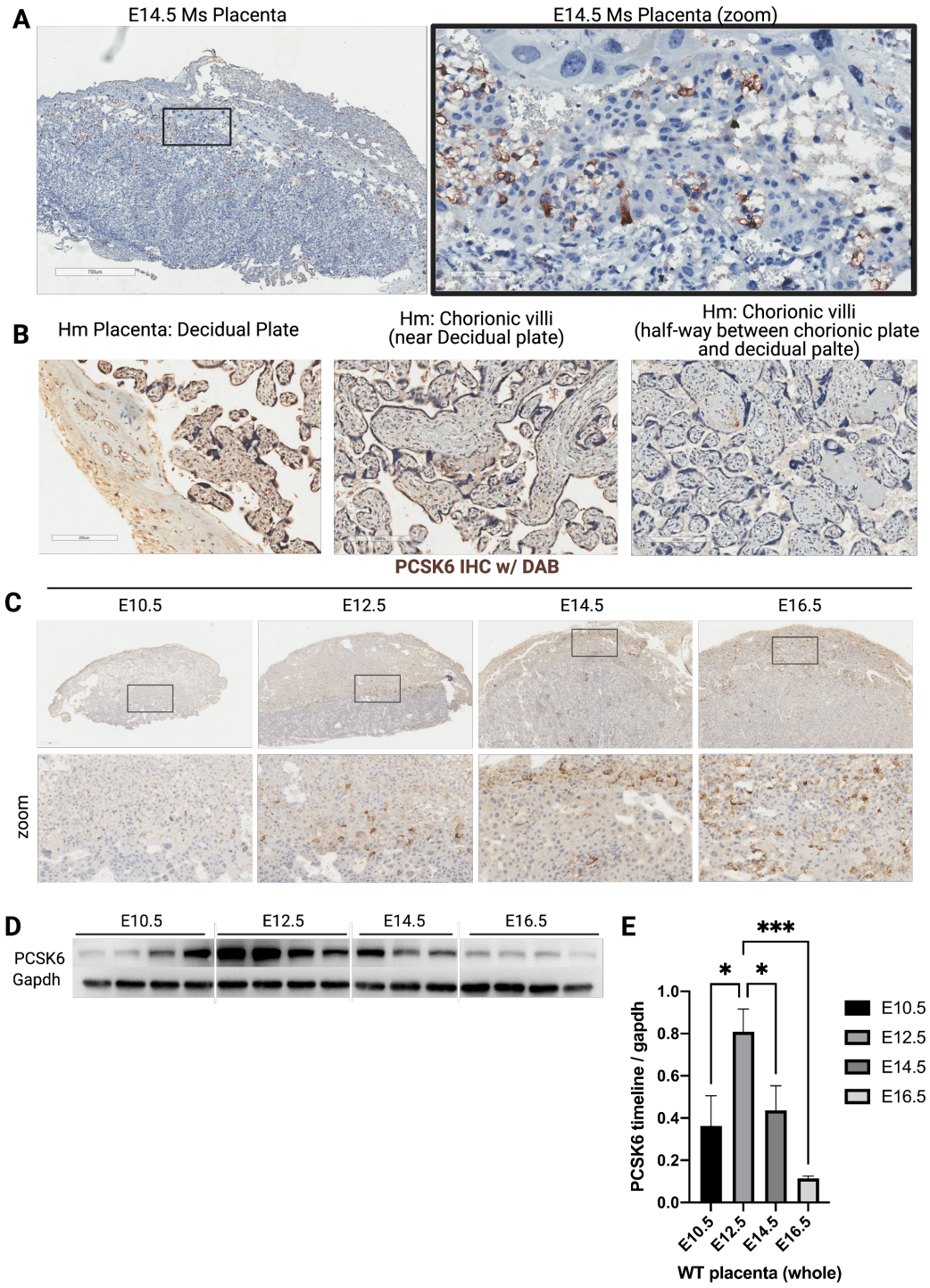

Figure 8. PCSK6 is dynamically regulated in the mouse placenta. (A) Mouse (Ms) placenta at E14.5 with PCSK6 visualized with DAB. (B) Term human (Hm) placenta with PCSK6 visualized with DAB. (C) PCSK6 visualized with DAB overtime. (D) Transient PCSK6 expression in whole Ms placenta lysate detected via WB. (E) Analysis of PCSK6 expression in Ms placenta detected by WB (n=3-4 per group, One-way ANOVA p=0.0046, Brown-Forsyth test p=0.1815). Created with BioRender.com.

PCSK6 expression in mouse placenta decreased under HG

STZ-induced hyperglycemic mouse placentas from E14.5 were micro-dissected to separate Lab and Jz+Db. These tissue samples were used for western blot detection of PCSK6. In hyperglycemic placentas, PCSK6 expression decreased in both the Lab and Jz+Db placenta lysates (Fig 9A-C).

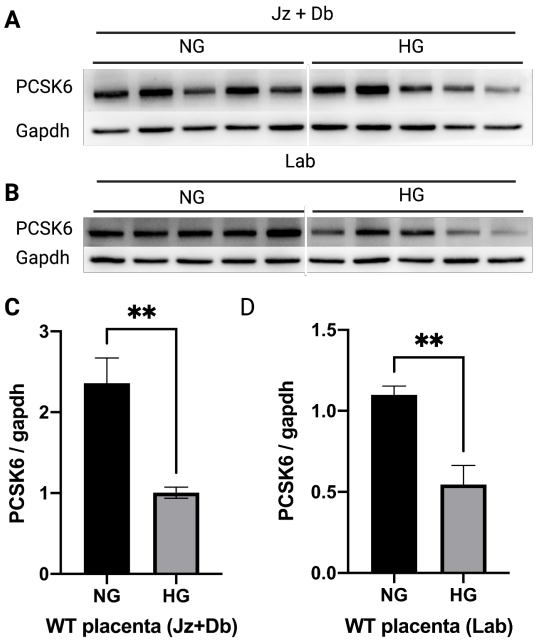

Figure 9. PCSK6 protein expression decreases in both the Lab and Jz+Db layer of hyperglycemic placenta. (A,C) WB results of PCSK6 expression in hyperglycemic Jz+Db tissue sample. (B,D) WB results of PCSK6 expression in hyperglycemic Lab tissue sample. n=5 group. Created with BioRender.com.

PCSK6 KO decreased embryo weight, and its interaction with hyperglycemia decreased placenta weight

The maternal age and weight at mating were similar across all groups (Fig 10A,B). STZ treatment successfully induced GDM by raising blood glucose to hyperglycemic levels after mating (Fig 10C). Maternal blood glucose became significantly higher by E7.5 and remained at

high levels until sacrifice at E14.5 in the STZ groups compared to their euglycemic counterparts (Fig 10C). At E14.5, the blood glucose of maternal KO-H group became significantly higher than that of the WT-H group (Fig 10C). At collection, amniotic fluid glucose levels were measured. Two-way ANOVA revealed that STZ-treatment, PCSK6 KO, and their interaction significantly altered the amniotic fluid glucose levels (Table 4). Consistent with the maternal blood glucose, the STZ-treated HG embryo groups—WT-H and KO-H, had significantly higher glucose concentrations in their amniotic fluid compared to their NG counterparts (Fig 10D). The KO-H embryos had significantly higher glucose levels compared to the WT-H embryos (Fig 10D).

Two-way ANOVA analysis revealed that the litter size was not significantly affected by hyperglycemia or *PCSK6 KO* alone, but was influenced by the interaction of the two factors (Table 4). The litter size was marginally increased in the KO-H litter compared to the KO litter (Fig 10E). The embryo weight at E14.5 was affected by hyperglycemia and *PCSK6 KO* (Table 4). Embryo weight was lower in the hyperglycemic groups and was the lowest in the KO-H group (Fig 10F). Hyperglycemia and its interaction with *PCSK6 KO* influenced placenta weight (Table 4). While the KO group had increased placenta weight, that of the KO-H group decreased (Fig 10G).

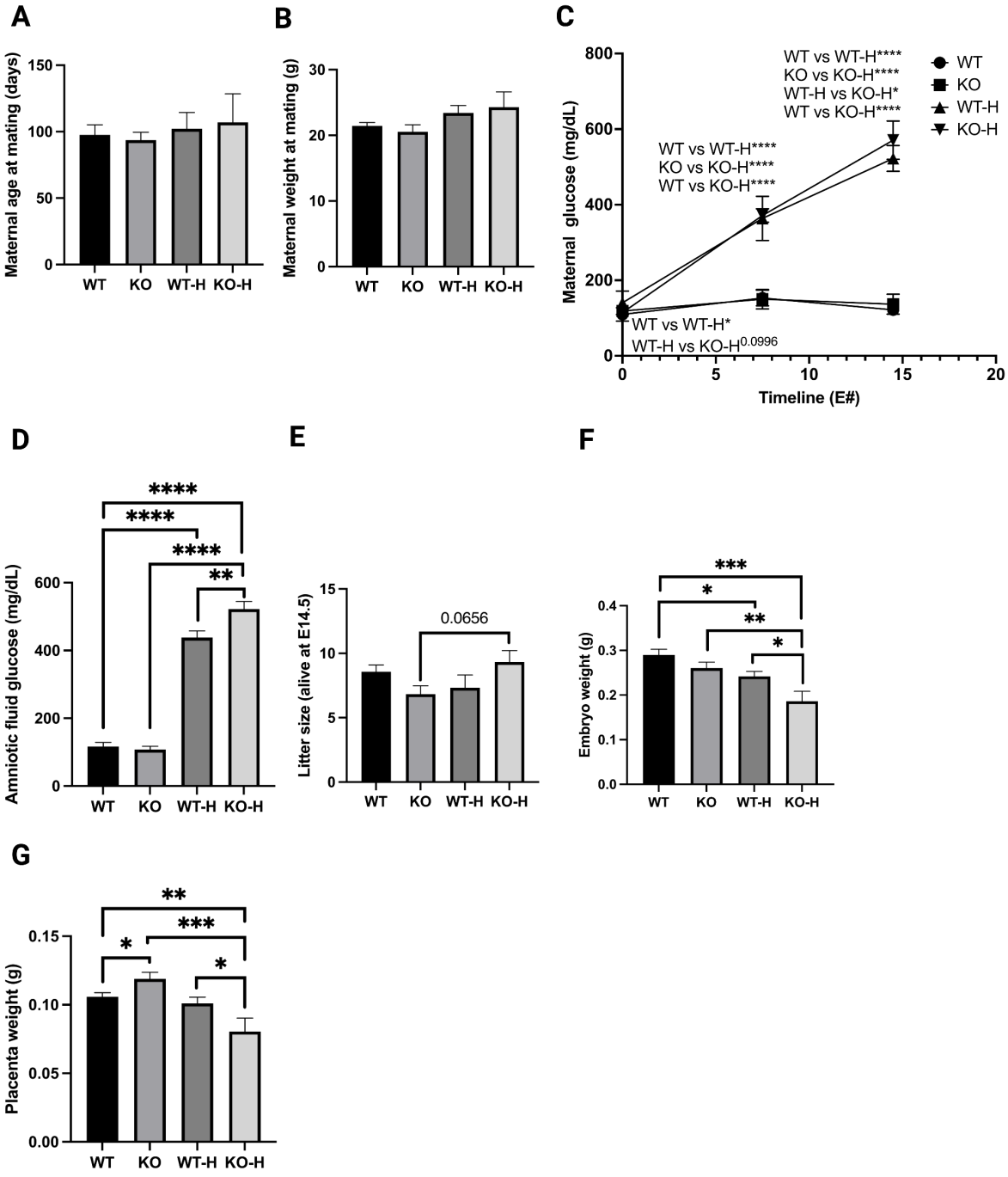

Figure 10. *PCSK6 KO* decreased embryo weight, and its interaction with hyperglycemia decreased placenta weight. (A) Maternal age at mating (m=3-7 per group). (B) Maternal weight at mating (m=3-7 per group). (C) Maternal glucose change overtime from mating, E7.5, and E14.5 at the time of sacrifice (m=2-7 per group). (D) Amniotic fluid glucose concentration at the time of collection (m=7 per group). (E) Litter size of embryos alive at E14.5 (m=3-7 per group). (F). Embryo weight at E14.5 (m=3-7 per group). (G) Placenta weight at E14.5. Fisher LSD's p-values are noted as *($p<0.05$), **($p<0.01$), ***($p<0.001$), ****($p<0.0001$). Created with BioRender.com.

Table 4. Two-way ANOVA results for pregnancy data. Results of the test are reported as p-values noted as ns (p>0.1), *(p<0.05), **(p<0.01), ***(p<0.001), ****(p<0.0001).

2-way ANOVA	Amniotic fluid glucose	Litter size	Embryo weight	Placenta weight
Hyperglycemia effect	****	ns	***	***
***PCSK6 KO* effect**	*	ns	**	ns
Interaction	*	*	ns	**

Embryos from PCSK6 KO-H pregnancies had a lower genotype frequency of *PCSK6 KO*

Our mouse model consisted of a *PCSK6+/-* crossed with either *PCSK6 WT* or *KO*. Therefore, all offspring genotype prevalence from any of the pregnancy group should be around 50% each. Genotyping of the embryos revealed that the proportion of *PCSK6 KO* embryo genotype is significantly lower compared to other genotype proportions (Table 5). However, we also observed that KO-H pregnancies had a larger litter size (alive at E14.5). This inconsistency may be due to the KO-H group being sampled from only three pregnancies (KO-H m=3).

Table 5. The proportion of *PCSK6 KO* embryos was lower compared to genotype proportion of other litters. Results of the $\chi 2$ test are reported as p-values noted as ns (p>0.1), *(p<0.05), **(p<0.01), ***(p<0.001), ****(p<0.0001).

Mother Group	Embryo genotype		$\chi 2$ test p-value
	PCSK6 +/-	***PCSK6 WT***	
WT	**30**	**30**	
WT-H	**21**	**23**	**ns (vs WT)**
	PCSK6 +/-	***PCSK6 KO***	
KO	**21**	**20**	**ns (vs WT)**
KO-H	**20**	**8**	**0.0587 (vs WT)** **0.0932 (vs KO)** *** (vs WT-H)**

Incidence of neural tube & craniofacial defects increased in PCSK6 KO-H embryos

Embryos were assessed for neural tube and craniofacial defects. All WT samples appeared to be normal (Fig 11A and C), while the KO and KO-H group had embryos with neural

tube (Fig 11 E,G,H) and craniofacial defects (Fig 11E-H). Simple logistic regression showed that neural tube and craniofacial defect rate was affected by the interaction between *PCSK6 KO* and hyperglycemia (Table 6). The same test showed that *PCSK6 KO* and hyperglycemia, independently, do not affect the incidence of neural tube and craniofacial defects. Based on the $\chi 2$ test, only the KO-H group was deemed to increase the incidence of neural tube and craniofacial defects compared to the WT group (Table 7). Note that the embryos from the KO and KO-H group have no pigment in their eyes (Fig 11 B,D,E-H), which is a specific phenotype of *PCSK6 KO* mice. There were no limb defects observed amongst any of the groups.

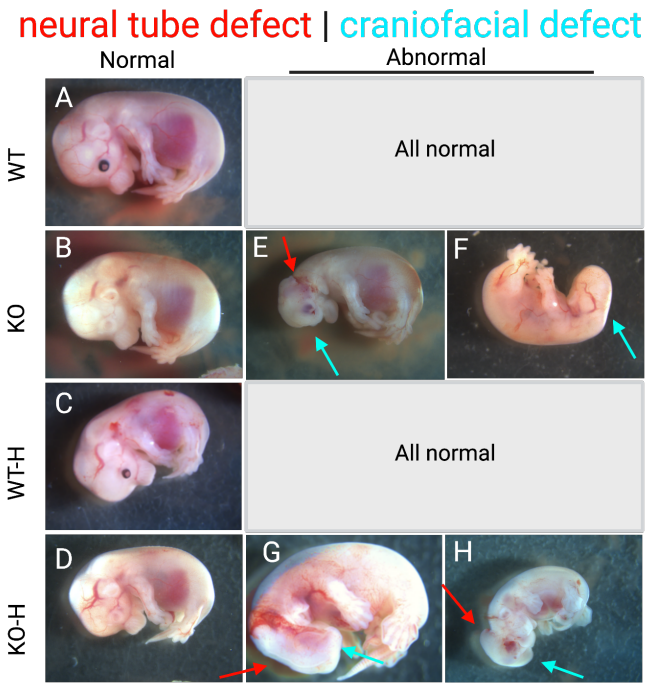

Figure 11. *PCSK6 KO* resulted in cases of neural tube and craniofacial defects and its interaction with hyperglycemia significantly increased its incidence. (A-D) Embryos with normal appearances. (E,G,H) Embryos with neural tube defects indicated by red arrows. (E-H) Embryos with craniofacial defects indicated by blue arrows. NOTE: Image G was taken at 1.0x while others were taken at 0.73x. Created with BioRender.com.

Table 6. Simple logistic regression test on the effect of hyperglycemia, *PCSK6 KO*, and their interaction on neural tube and craniofacial defects. Likelihood ratio test was performed, and results were listed as ns (p>0.1), *(p<0.05), **(p<0.01), ***(p<0.001), ****(p<0.0001).

Simple logistic regression / Likelihood ratio test	Craniofacial	Neural tube
Hyperglycemia effect	ns	ns
***PCSK6 KO* effect**	ns	ns
Interaction effect	*	*

Table 7. Summary of defects and χ2 test results of assessed defects. Results of the test are reported as p-values noted as ns (p>0.1), *(p<0.05), **(p<0.01), ***(p<0.001), ****(p<0.0001).

	Neural tube			Craniofacial		
Embryo Group	Defect	Normal	χ2 test p-value	Defect	Normal	χ2 test p-value
WT	0	30		0	30	
KO	1	19	ns (vs WT)	2	19	0.0771 (vs WT)
WT-H	0	23	ns (vs WT)	0	23	ns (vs WT)
KO-H	2	5	**(vs WT) ns (vs KO) *(WT-H)	2	5	**(vs WT) ns (vs KO) *(vs WT-H)

Hyperglycemia increased the incident of outflow tract defects

Embryo hearts were sectioned and analyzed for impression of left ventricle hyper-trabeculation and presence of outflow tract (OFT) defects, such as overriding aorta (OA) and double outlet right ventricle (DORV). The interaction between *PCSK6 KO* and hyperglycemia was found to affect the incidence of DORV and combined OFT defects (Table 8). OA was observed in WT-H and KO-H groups, but was not considered a significant increase in its incidence (Fig 12H,L and Table 9). DORV was observed in WT-H and KO-H groups but was considered a marginal increase only for KO-H (Fig 12I,M). OFT defects combined, the WT-H group had a marginal increase compared to WT while the KO-H group had a significant increase in incident compared to both WT and KO groups (Table 9).

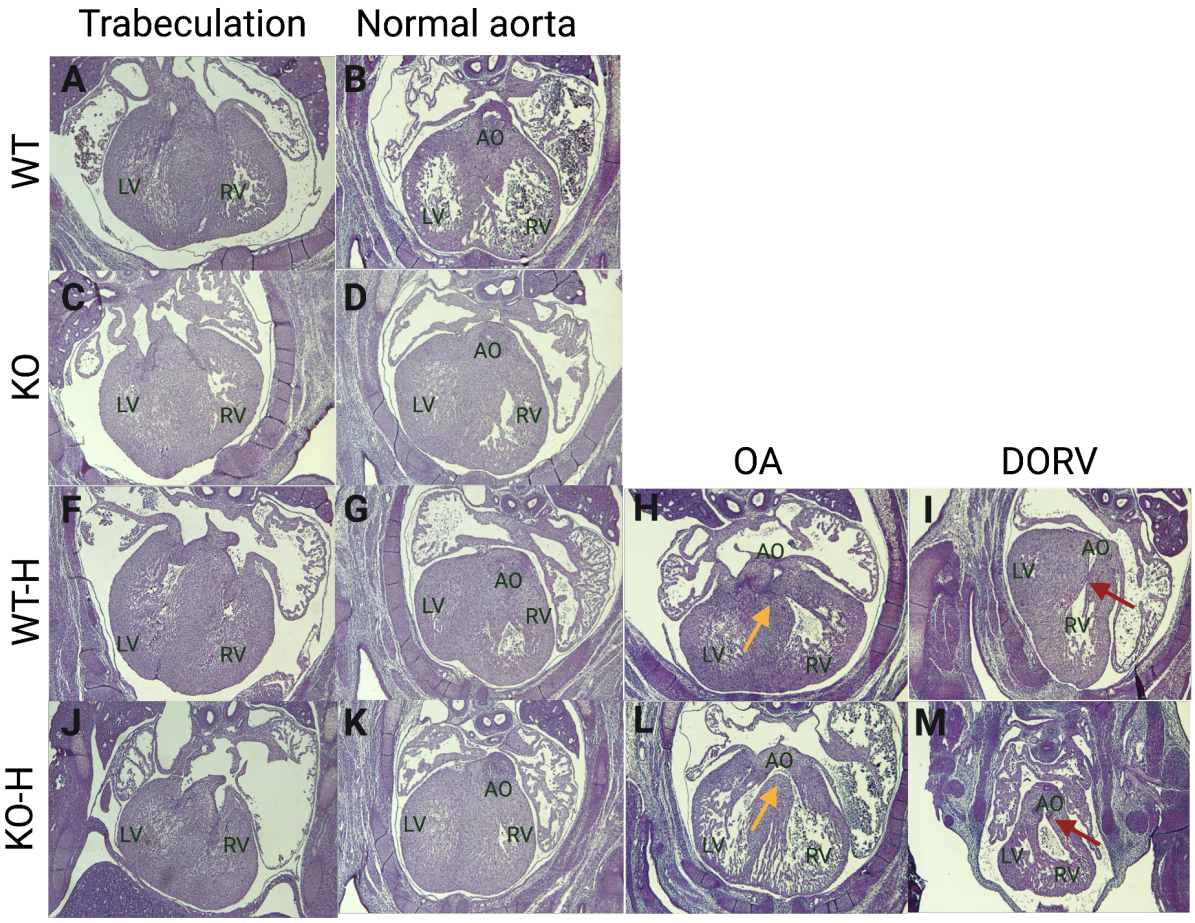

Figure 12. Hyperglycemia increased the incident of outflow tract defects. (A,C,F,J) view used for classification of hyper-trabeculation. (B,D,G,K) Images of normal aorta. (H,L) Image of OA indicated by yellow arrows. (I,M) Images of DORV indicated by red arrows. AO = aorta. Created with BioRender.com.

Table 8. Simple logistic regression test on the effect of hyperglycemia on out flow tract defects. Likelihood ratio test was performed, and results were listed as ns ($p>0.1$), *($p<0.05$), **($p<0.01$), ***($p<0.001$), ****($p<0.0001$).

Simple logistic regression / Likelihood ratio test	LV hyper-trabeculation	OA	DORV	OFT combined
Hyperglycemia effect	ns	ns	ns	ns
***PCSK6 KO* effect**	ns	ns	ns	ns
Interaction effect	ns	ns	0.0989	0.0548

Table 9. Recorded incidence of heart defects. $\chi 2$ test was performed and results were listed as ns (p>0.1), *(p<0.05), **(p<0.01), ***(p<0.001), ****(p<0.0001).

χ2 test	**LV hyper-trabeculation**			**OA**		
Embryo Group	Hyper-trabeculated	Normal	p-value	Defect	Normal	p-value
WT	4	2		0	6	
KO	3	4	ns (vs WT)	0	7	ns (vs WT)
WT-H	4	1		1	4	ns (vs WT)
KO-H	3	3	ns (vs WT) ns (vs KO) ns (vs WT-H)	1	5	ns (vs WT) ns (vs KO) ns (vs WT-H)
χ2 test	**DORV**			**OFT combined**		
Embryo Group	Defect	Normal	p-value	Defect	Normal	p-value
WT	0	6		0	6	
KO	0	7	ns (vs WT)	0	7	ns (vs WT)
WT-H	1	4	ns (vs WT)	2	3	0.0868 (vs WT)
KO-H	2	4	ns (vs WT) 0.0968 (vs KO) ns (vs WT-H)	3	3	* (vs WT) * (vs KO) ns (vs WT-H)

Overall placenta morphology

Hyperglycemia, but not PCSK6 KO, increased GlyT area within Jz

The placenta layer distribution was analyzed on PAS staining (Fig 13A). Hyperglycemia affected Db size, and marginally and significantly increased the size of Db layer in both WT and *PCSK6 KO* placenta, respectively (Fig 13B, Table 10). Jz and Lab size, and Lab / Jz ratio was not affected by hyperglycemia, *PCSK6 KO*, nor their interaction (Fig 13C-E).

Within the Jz, free-hand selections of areas comprising of different cell types were made. The GlyT areas were selected based on ballooning and/or clusters of cells heavily pigmented with PAS-stained glycogen granules. The two-way ANOVA test revealed that hyperglycemia impacts the ratio of GlyT area within the Jz with no significant effect on the SpT area (Table 10).

Fisher LSD revealed that GlyT area increased in WT-H and KO-H compared to their normo-glycemic counterparts (Fig 13F). SpT area was not affected by hyperglycemia, *PCSK6 KO*, nor their interaction (Table 10, Fig 13G). Overall, hyperglycemia, but not *PCSK6 KO*, increased the GlyT area within the Jz (Table 10).

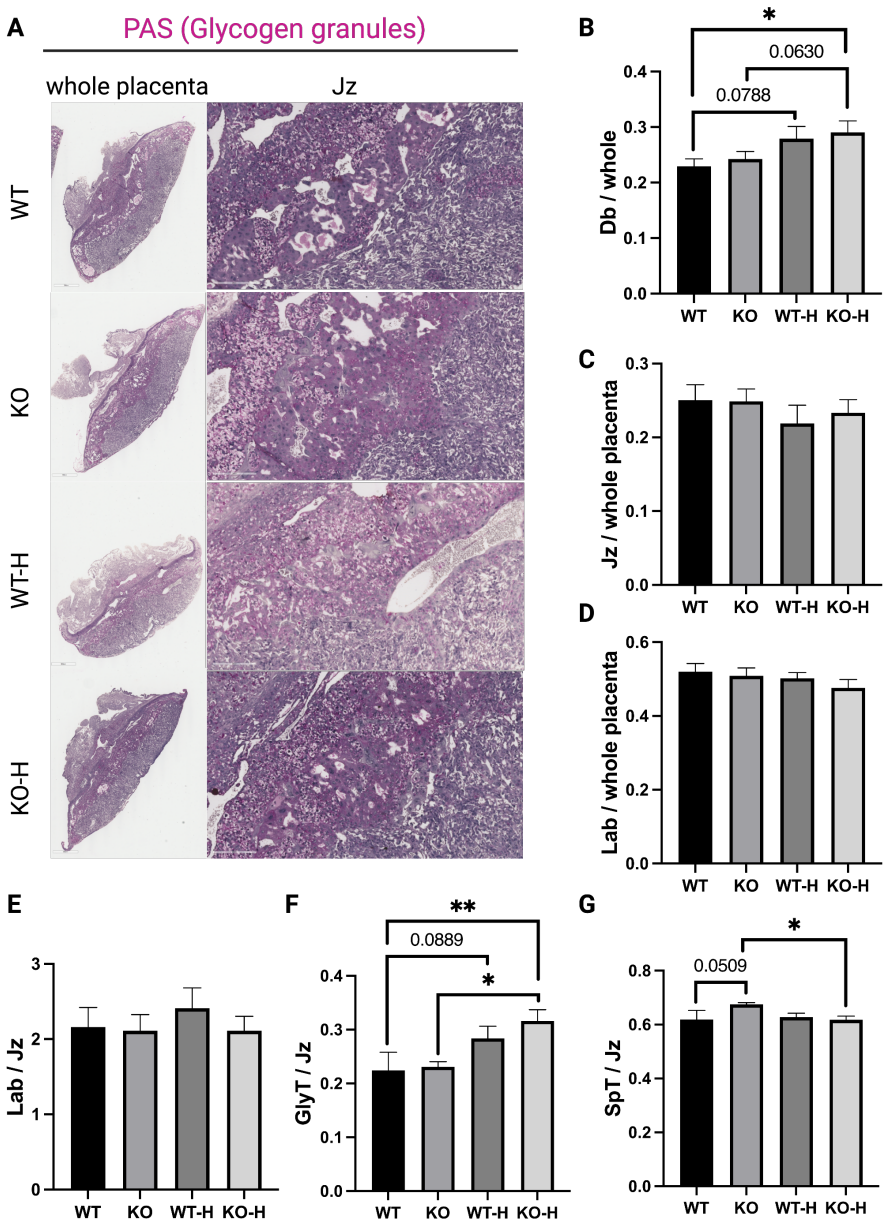

Figure 13. Hyperglycemia, but not *PCSK6 KO*, increased GlyT area relative to Jz. (A) PAS staining. (B) Db area / whole placenta area. (C) Jz area / whole placenta area. (D) Lab area / whole placenta area. (E) Lab area relative to Jz area. (F) Total area of GlyTs in the Jz. (G) SpT area in the Jz. Fisher LSD's p-values are noted as *($p<0.05$), **($p<0.01$), ***($p<0.001$), ****($p<0.0001$). n=5-6 from m=3-5 per group. Created with BioRender.com.

Table 10. Two-way ANOVA results for placenta morphometric measurements. Results of the test are reported as p-values noted as ns (p>0.1), *(p<0.05), **(p<0.01), ***(p<0.001), ****(p<0.0001).

2-way ANOVA	**Db area / whole**	**Jz area / whole**	**Lab area / whole**	**Lab / Jz**	**GlyT / Jz**	**SpT / Jz**
Hyperglycemia effect	*	ns	ns	ns	**	ns
***PCSK6 KO* effect**	ns	ns	ns	ns	ns	ns
Interaction	ns	ns	ns	ns	ns	ns

The observed increase in GlyT area within the Jz of hyperglycemic groups in the PAS staining was further investigated by performing an IF staining of trophoblast-specific protein α (Tpbpα). Tpbpα stains cells of the Jz with the greatest intensity in the SpT and a rather faint staining in GlyTs (Fig 14A). Using the Image J software, the Jz area and GlyT occupying areas were selected and used to quantify the cell number in each of those respective areas. The total area occupied by GlyTs in the Jz area showed an increase caused by hyperglycemia (Table 11). This result was consistent with that of the PAS staining (Fig 13F and Fig 14B). Within the selected GlyT areas, Dapi stained nuclei were counted and compared to the total cell count within the Jz. Hyperglycemia, but not PCSK6 deletion, increased the GlyT cell count relative to all cell types in the Jz (Fig 14C, Table 11). Then, we took the total area of the GlyT area selections and divided it with the GlyT nuclei count to calculate the GlyT cell size. This calculated GlyT cell size itself did not change (Fig 14D, Table 11). In addition to the absence of change in GlyT cell size, the total cell # of the Jz did not change (Fig 14E). Therefore, it can further be suggested that the increased GlyT number comes from increased differentiation of Tpbpα+ cells into GlyTs.

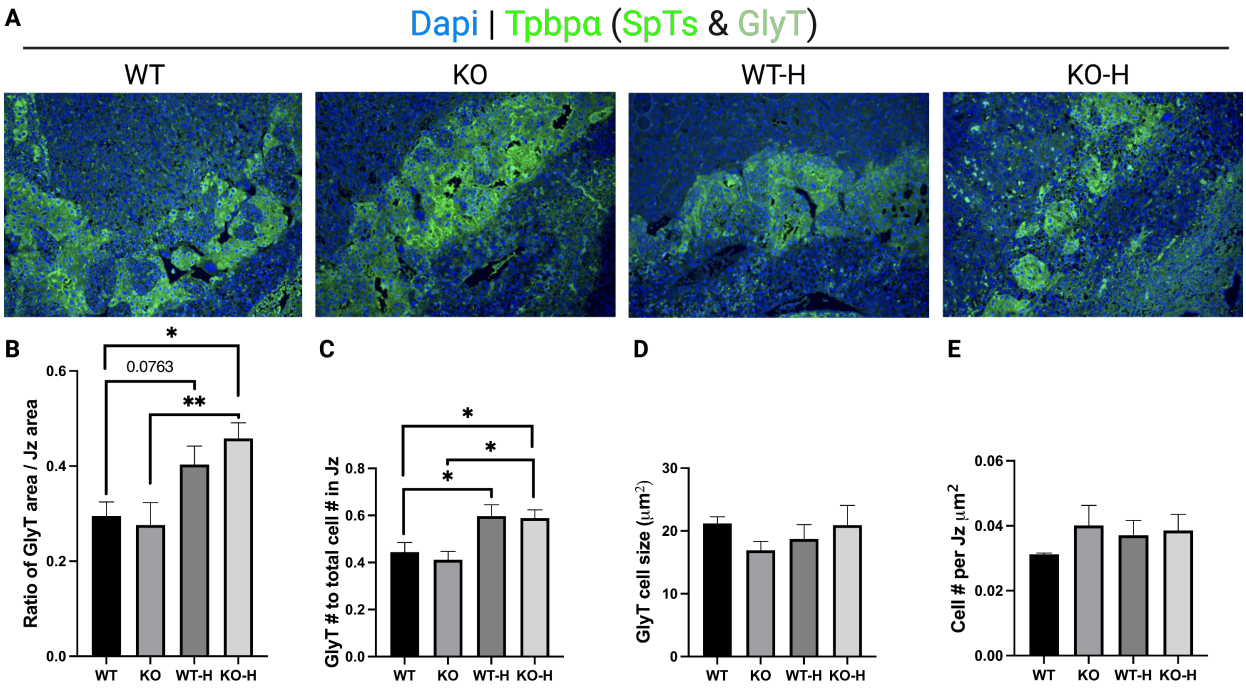

Figure 14. Increase in GlyT area is caused by increased GlyT cell ratio. (A) Tpbpα staining visualizes the Jz and different cell types within. The intense staining represents SpTs, while relatively faint areas represent GlyTs. (B) GlyT area over Jz area. (C) Number of GlyTs to total cell count in Jz. (D) GlyT cell size. (E) Number of all cells in the Jz divided by Jz area. Fisher LSD's p-values are noted as *(p<0.05), **(p<0.01), ***(p<0.001), ****(p<0.0001). (n=3 from m=3 per group). Created with BioRender.com.

Table 11. Two-way ANOVA results for parameters analyzed on Tpbpα images. Results of the test are reported as p-values noted as ns (p>0.1), *(p<0.05), **(p<0.01), ***(p<0.001), ****(p<0.0001).

2-way ANOVA	GlyT area / Jz area	GlyT # to total cell # in Jz	GlyT cell size	# of all cells in Jz / area
Hyperglycemia effect	**	**	ns	ns
***PCSK6 KO* effect**	ns	ns	ns	ns
Interaction	ns	ns	ns	ns

Placenta fibrosis and cell proliferation at E14.5 were not affected by PCSK6 KO or hyperglycemia

Sirius Red staining did not show any noticeable sign of fibrosis in any of the groups (Fig 15A). On E14.5 placentas, p-H3S10+ cell count was very low, and, if present, were found mostly in the Lab region with little or none in the Jz and Db (Fig 15B). The count of the p-H3S10+ cells was too small to have any biological significance.

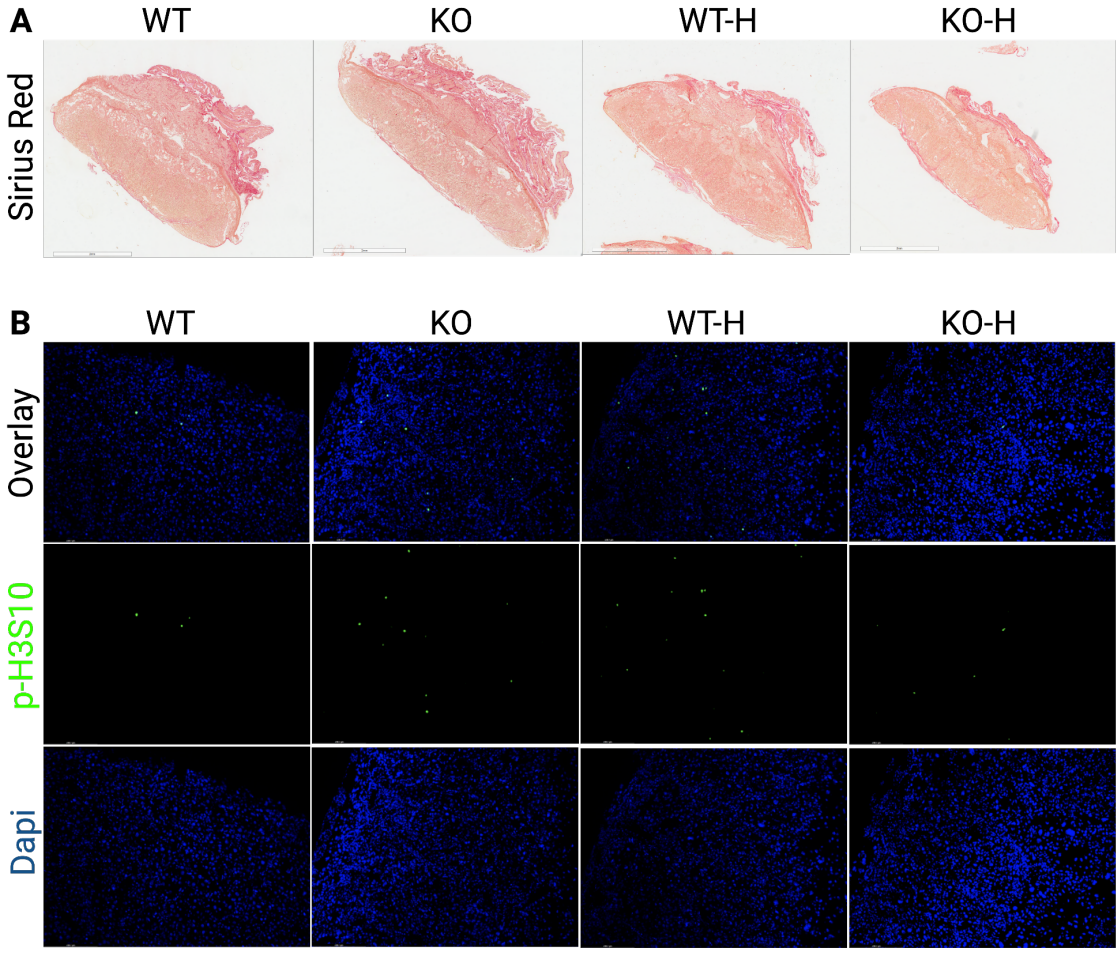

Figure 15. Placenta fibrosis and proliferation are not affected by *PCSK6 KO*, hyperglycemia, or its interaction. (A) Sirius Red staining. (B) p-H3S10 IF of Lab. Created with BioRender.com.

PCSK6 KO hindered the SpA remodeling process

PCSK6 KO decreased SpA LD and LD / OD ratio

SpA remodeling was assessed in two methods: by looking at the SpA diameter and looking at TGC association with the SpA itself. From the HE staining, we investigated the size of SpA lumen (LD) and outer diameter (OD) (Fig 16A). The two-way ANOVA analysis showed that LD was significantly affected by *PCSK6 KO* and marginally affected by its interaction with hyperglycemia (Table 12). LD was significantly shorter in KO placentas and marginally so in KO-H placentas compared to WT (Fig 16B). The degree of SpA vascular remodeling was determined by LD to OD ratio. *PCSK6 KO* and its interaction with hyperglycemia affected LD/OD ratio which resulted in decreased LD/OD ratio in the KO and KO-H placentas compared to the WT placentas (Table 12, Fig 16C).

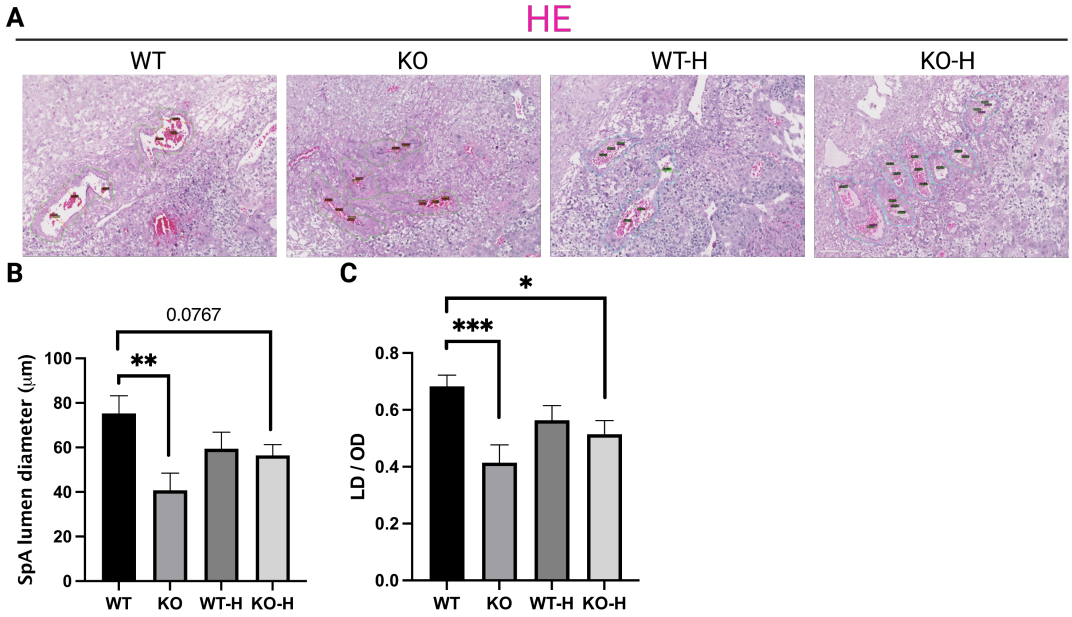

Figure 16. *PCSK6 KO* decreased SpA LD and LD / OD ratio. (A) HE staining of SpAs residing in the distal portion of Db layer. (B) SpA lumen diameter. (C) SpA vascular remodelness of SpA indicated by LD / OD ratio. Fisher LSD's p-values are noted as *($p<0.05$), **($p<0.01$), ***($p<0.001$), ****($p<0.0001$). n=4-7 from m=3-5 per group. Created with BioRender.com.

Table 12. Two-way ANOVA results for SpA LD and LD / OD ratio. Results of the test are reported as p-values noted as ns (p>0.1), *(p<0.05), **(p<0.01), ***(p<0.001), ****(p<0.0001).

2-way ANOVA	**SpA LD**	**SpA LD / OD**
Hyperglycemia effect	ns	ns
***PCSK6 KO* effect**	*	**
Interaction	**0.0534**	*

PCSK6 KO decreased TGC association with SpAs

TGC association was assessed, single-blinded, using Co-IF staining of Cytok and PECAM. Cytok stains all trophoblast cells including the TGCs, and PECAM stains the endothelial cells of the SpA (Fig 17). Each SpA was given a category based on the degree of TGC association: full (75%=<), partial (25~75%), or none. If more than 50% of the SpAs in a single placenta had either full or partial TGC association, that placenta was given a category of "TGC-associated". TGC association was affected by *PCSK6 KO* (Table 13). The $\chi 2$ test revealed that the KO and KO-H groups had decreased TGC association compared to the WT group (Table 14).

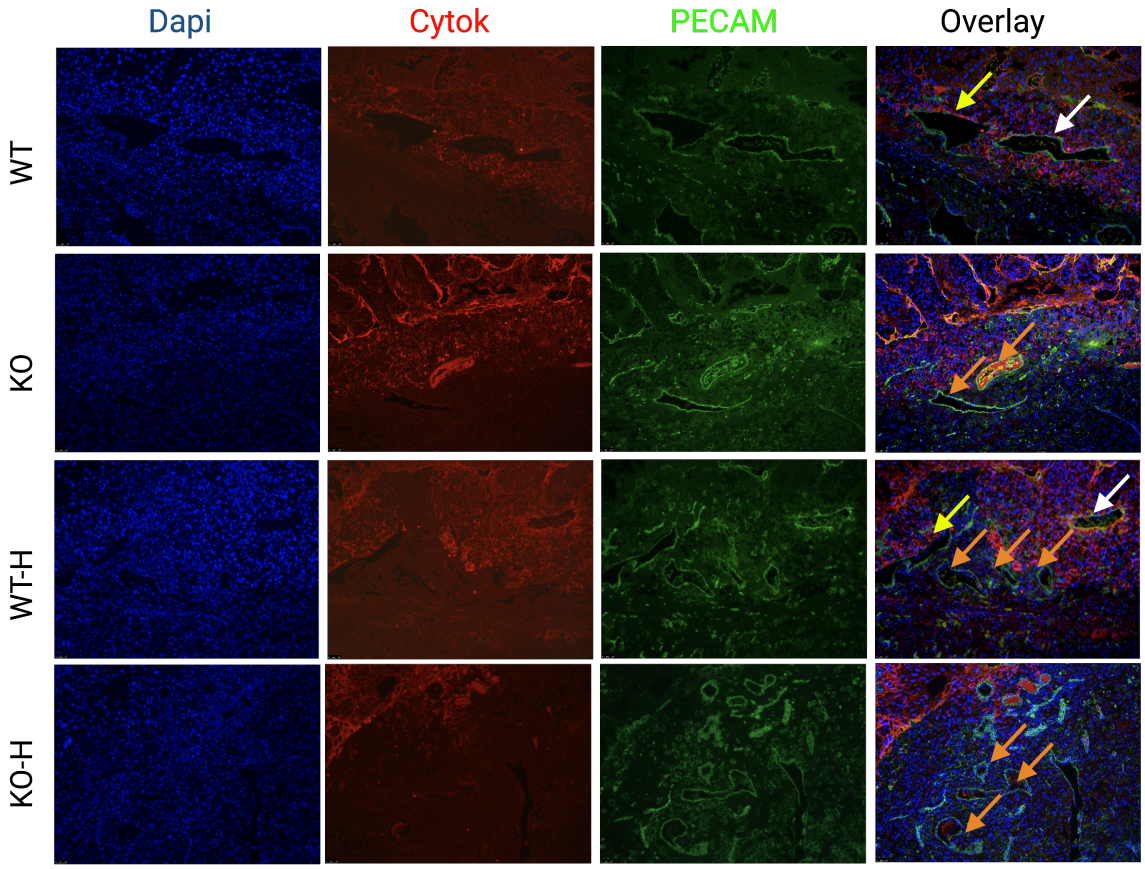

Figure 17. *PCSK6 KO* and hyperglycemia decreased TGC association with SpAs in the distal Db. (A) Image of SpAs with TGCs visualized with cytok. (B) Graph visualizing the classification of TGC association. n=5-6 from m=3-5 per group. White arrows indicate full association. Yellow arrows indicate partial association. Orange arrows indicate non-associated SpAs. Created with BioRender.com.

Table 13. Simple logistic regression test on the effect of hyperglycemia, *PCSK6 KO*, and their interaction on SpA-TGC association. Likelihood ratio test was performed, and results were listed as ns (p>0.1), *(p<0.05), **(p<0.01), ***(p<0.001), ****(p<0.0001).

Simple logistic regression / Likelihood ratio test p-value	SpA-TGC association
Hyperglycemia effect	**ns**
***PCSK6 KO* effect**	*****
Interaction effect	**ns**

Table 14. Classification of TGC association. $\chi 2$ test was performed and results were listed as ns ($p>0.1$), *($p<0.05$), **($p<0.01$), ***($p<0.001$), ****($p<0.0001$).

$\chi 2$ test	TGC-associated	not associated	SpA-TGC association
WT	**5**	**1**	
KO	**1**	**4**	*** (vs WT)**
WT-H	**2**	**3**	**ns (vs WT)**
KO-H	**1**	**4**	*** (vs WT)** **ns (vs KO)** ns (vs WT-H)

Hyperglycemia suppressed the secretion of latent TGFβ1 while both hyperglycemia and PCSK6 KO decreased mature TGFβ1 levels

We then performed WB to see if expression of proteins regulating TGC migration and invasion were altered by *PCSK6 KO*, hyperglycemia, or their interaction. TGFβ1 is an inhibitor of cell migration in multiple placenta cell line studies.[33,34] Two-way ANOVA tests suggested that hyperglycemia affected both mature and latent TGFβ1, while *PCSK6 KO* only affected mature TGFβ1 levels (Table 15). Both mature and latent TGFβ1 were down-regulated in the WT-H, and KO-H placentas compared to that of WT group (Fig 18). KO-H group also had significantly downregulated mature and latent TGFβ1 compared to the KO group (Fig 18). The KO-H placentas had marginally decreased mature TGFβ1 compared to the WT-H placenta (Fig 18).

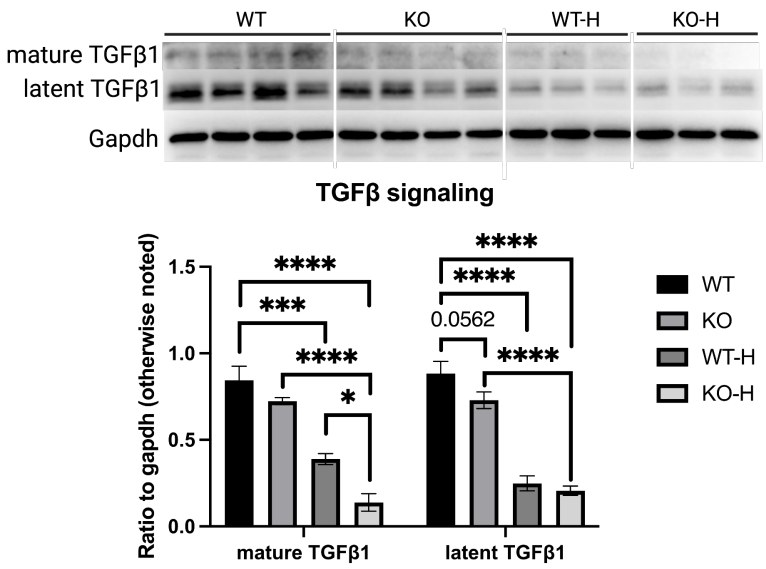

Figure 18. Latent TGFβ1 secretion is decreased in hyperglycemic groups while the suppression of mature TGFβ1 is greatest in the KO-H. Fisher LSD's p-values are noted as *(p<0.05), **(p<0.01), ***(p<0.001), ****(p<0.0001). n=3-4 from m=3-4 per group. Created with BioRender.com.

Table 15. Two-way ANOVA results for TGFβ1 protein expression. Results of the test are reported as p-values noted as ns (p>0.1), *(p<0.05), **(p<0.01), ***(p<0.001), ****(p<0.0001).

2-way ANOVA	**mature TGFβ1**	**latent TGFβ1**
Hyperglycemia effect	****	****
***PCSK6 KO* effect**	**	ns
Interaction	ns	ns

PCSK6 KO increased phosphorylation of β-*catenin*

The impact of *PCSK6 KO* and hyperglycemia was also investigated on the canonical Wnt signaling proteins. Increased β-catenin levels have been implicated with migratory gene expressions.[37,38] Two-way ANOVA suggested that PCSK6 KO significantly affects the phospho(p)-β-catenin to total-β-catenin ratio (Fig 19, Table 16). Reflectively, the ratio of p-β-catenin to total-β-catenin levels were marginally and significantly increased in the KO and KO-

H, respectively (Fig 19). The total β-catenin levels were not significantly altered in any of the treatment groups (Fig 19). These results suggest an increase in the phosphorylation of β-catenin.

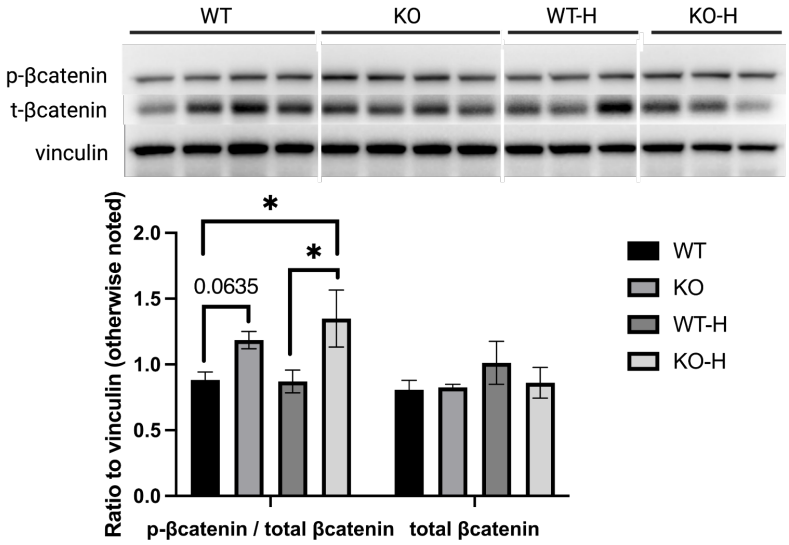

Figure 19. *PCSK6 KO* increased phosphorylation of β-catenin. Fisher LSD's p-values are noted as *(p<0.05), **(p<0.01), ***(p<0.001), ****(p<0.0001). n=3-4 from m=3-4 per group. Created with BioRender.com.

Table 16. Two-way ANOVA results for β-catenin protein expression. Results of the test are reported as p-values noted as ns (p>0.1), *(p<0.05), **(p<0.01), ***(p<0.001), ****(p<0.0001).

2-way ANOVA	**p-β-catenin / total-β-catenin**	**total-β-catenin**
Hyperglycemia effect	ns	ns
***PCSK6 KO* effect**	**	ns
Interaction	ns	ns

PCSK6 KO resulted in opposite angiogenic response based on glucose conditions

Next, the Lab angiogenesis was assessed in two ways: blood space and pericyte development. The blood space analysis allowed for investigating the degree of branching during angiogenesis while the pericyte assessment provided insights into the maturation of the fetal vessels in the placenta.

PCSK6 KO increased diffusion capacity under NG while the opposite occurred under hyperglycemia

Blood space was analyzed by tracing the fetal capillary and the maternal lacunae space. The PECAM stained the fetal capillaries and the Cytok stained all trophoblast cells in the Lab. Therefore, the maternal space was traced in areas that were enclosed by Cytok (Fig 20A). Each measurement of fetal capillary area (FCA) and maternal lacunae area (MLA) from an image was log-transformed before adding them up to get the sum to make the distribution closer to normal and minimize influence of outlier area sizes. This sum of log-transformed measurements was used to represent one sample and was statistically analyzed for the FCA and MLA graphs (Fig 20B-D). The blood space graphs were plotted with the sum of absolute measurements with significant marks from statistical tests performed on the log values. Two-way ANOVA suggested that FCA is influenced by *PCSK6 KO*, but Fisher LSD did not show significant differences between WT and KO under NG and HG (Table 17, Fig 20B). Two-way ANOVA revealed that MLA is affected by hyperglycemia, which showed as a significant difference between KO and KO-H with the Fisher LSD test (Table 17, Fig 20C). Total blood surface area, defined by the mean of FCA and MLA, was significantly affected by hyperglycemia (Table 17). Total blood surface area was marginally decreased in the KO-H group compared to the normo-glycemic KO group (Fig 20D).

IHM thickness was significantly affected by hyperglycemia and its interaction with *PCSK6 KO,* and was marginally affected by *PCSK6 KO* (Table 17). The Fisher LSD showed that KO-H placentas had thicker IHM compared to all other groups (Fig 20E). The calculated diffusion capacity was influenced by hyperglycemia and its interaction with *PCSK6 KO* (Table 17). Fisher LSD revealed that the diffusion capacity was decreased in KO-H compared to WT,

KO, and WT-H placentas (Fig 20F). In contrast, *PCSK6 KO* under normal glucose condition had increased diffusion capacity compared to the WT placentas (Fig 20F).

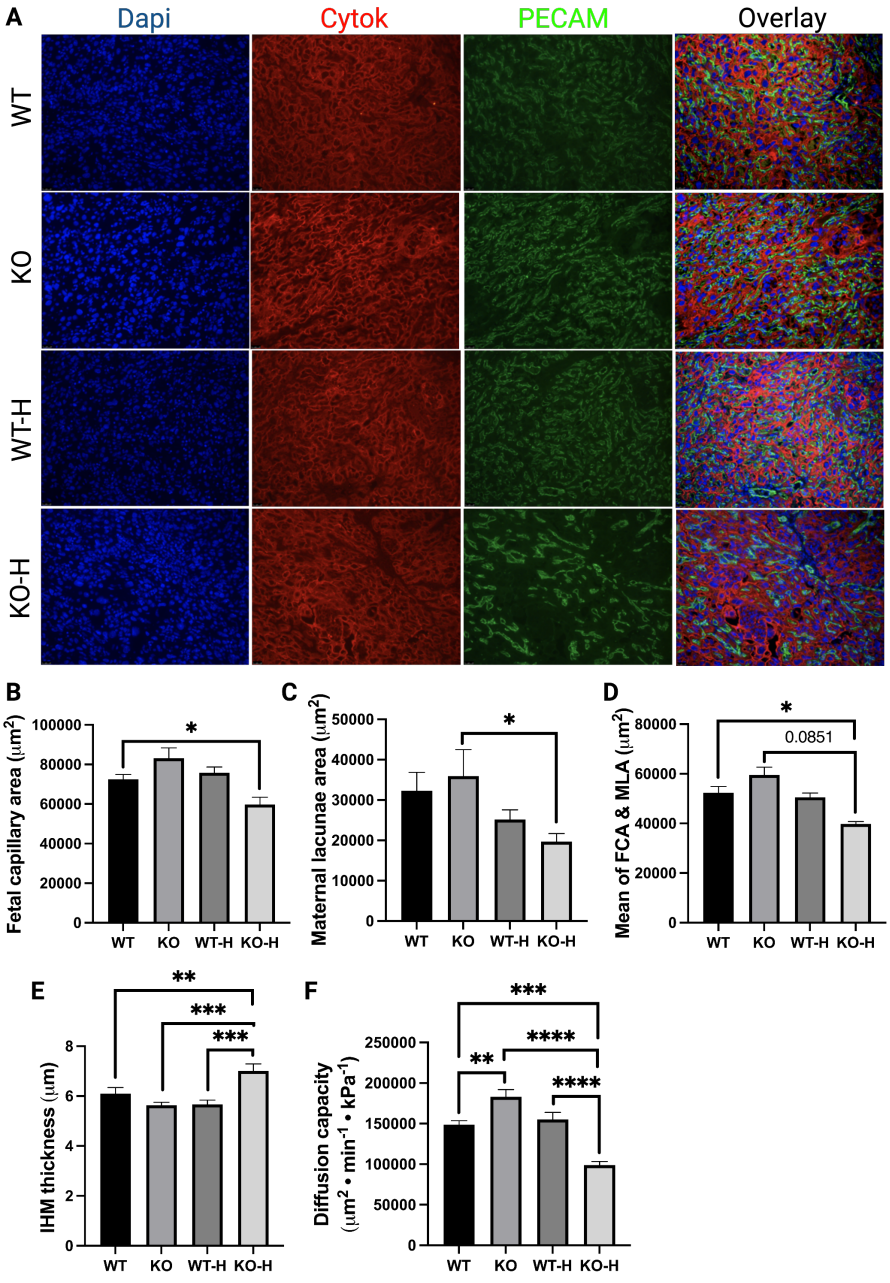

Figure 20. Blood space analysis revealed a glucose dependent angiogenesis among *PCSK6 KO* groups. (A) Co-IF of PECAM and Cytok in the Lab taken at 200x. (B-D) Area measurements of FCA, MLA, and the mean of FCA and MLA, respectively. (E) Thickness of IHM. (F) Calculated diffusion capacity. Fisher LSD's p-values are noted as *($p<0.05$),

(p<0.01), *(p<0.001), ****(p<0.0001). n=5 from m=3-5 per group. Created with BioRender.com.

Table 17. Two-way ANOVA results for blood space measurements. Results of the test are reported as p-values noted as ns (p>0.1), *(p<0.05), **(p<0.01), ***(p<0.001), ****(p<0.0001).

2-way ANOVA	Fetal capillary area	Maternal lacunae area	Mean FCA and MLA area	IHM	Diffusion capacity
Hyperglycemia effect	ns	*	*	*	****
***PCSK6 KO* effect**	*	ns	ns	0.0591	ns
Interaction	ns	ns	ns	***	****

PCSK6 KO-H Labyrinths have decreased expression of various angiogenic markers

Two-way ANOVA showed that *PCSK6 KO* affects insulin-like growth factor 1 receptor (IGF1R) expression while its interaction with hyperglycemia marginally affects VEGFA expression (Table 18). Hyperglycemia was shown to influence VEGFB, VEGFR1, VEGFR2, PDGFA, and PDGFC, PDGFRA, and PDGFRB mRNA expression in the Lab (Table 18). Except for VEGFR2, KO-H Labs had decreased expression of many angiogenic genes such as VEGFA, VEGFB, PDGFA, PDGFC, PDGFRB, and IGF1R (Fig 21).

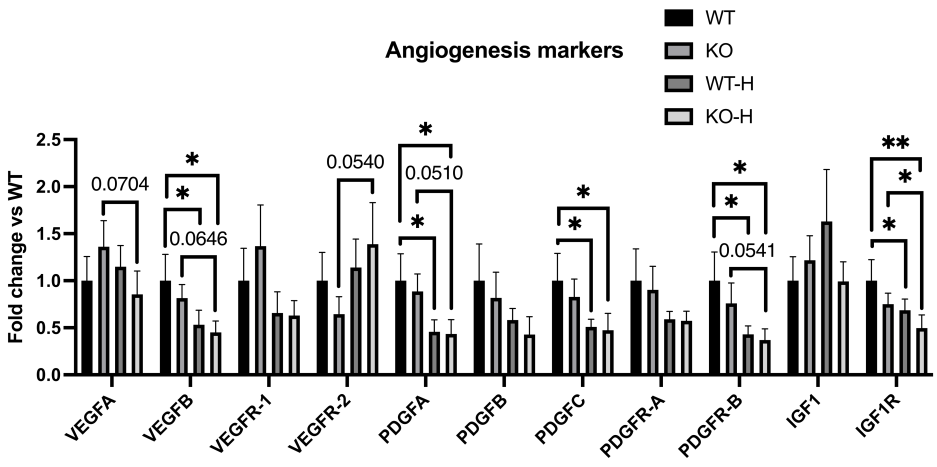

Figure 21. PCSK6 KO-H group had various angiogenic markers decreased due to hyperglycemia and/or *PCSK6 KO*. Fisher LSD's p-values are noted as *(p<0.05), **(p<0.01), ***(p<0.001), ****(p<0.0001). n=3-4 from m=3-4 per group.

Table 18. Two-way ANOVA results for angiogenic marker mRNA expression. Results of the test are reported as p-values noted as ns (p>0.1), *(p<0.05), **(p<0.01), ***(p<0.001), ****(p<0.0001).

2-way ANOVA	**VEGFA**	**VEGFB**	**VEGFR1**	**VEGFR2**	**PDGFA**	**PDGFB**	**PDGFC**	**PDGFR-A**	**PDGFR-B**	**IGF1**	**IGF1R**
Hyperglycemia effect	ns	*	0.0839	0.0906	**	ns	*	*	**	ns	**
***PCSK6 KO* effect**	ns	ns	ns	ns	ns	ns	ns	ns	ns	ns	*
Interaction	0.0826	ns	ns	ns	ns	ns	ns	ns	ns	ns	ns

PCSK6 KO-H labyrinths had decreased α-SMA+ *profiles*

Pericyte development on fetal capillaries was also investigated by co-IF staining of α-SMA and PECAM (Fig 22A). Two-way ANOVA suggested that the α-SMA+ profile was impacted by *PCSK6 KO*, which further interacted with hyperglycemia (Table 19). PCSK6 deletion did not affect the α-SMA+ profiles under NG (Fig 22B). However, they decreased under HG (Fig 22B). Hyperglycemia significantly enlarged the α-SMA+ profiles in WT placenta, but decreased α-SMA+ profiles in KO-H groups (Fig 22B). The α-SMA+ profile was ranked from the highest to the lowest as the follows: WT-H ≈KO≈WT>KO-H (Fig 22B).

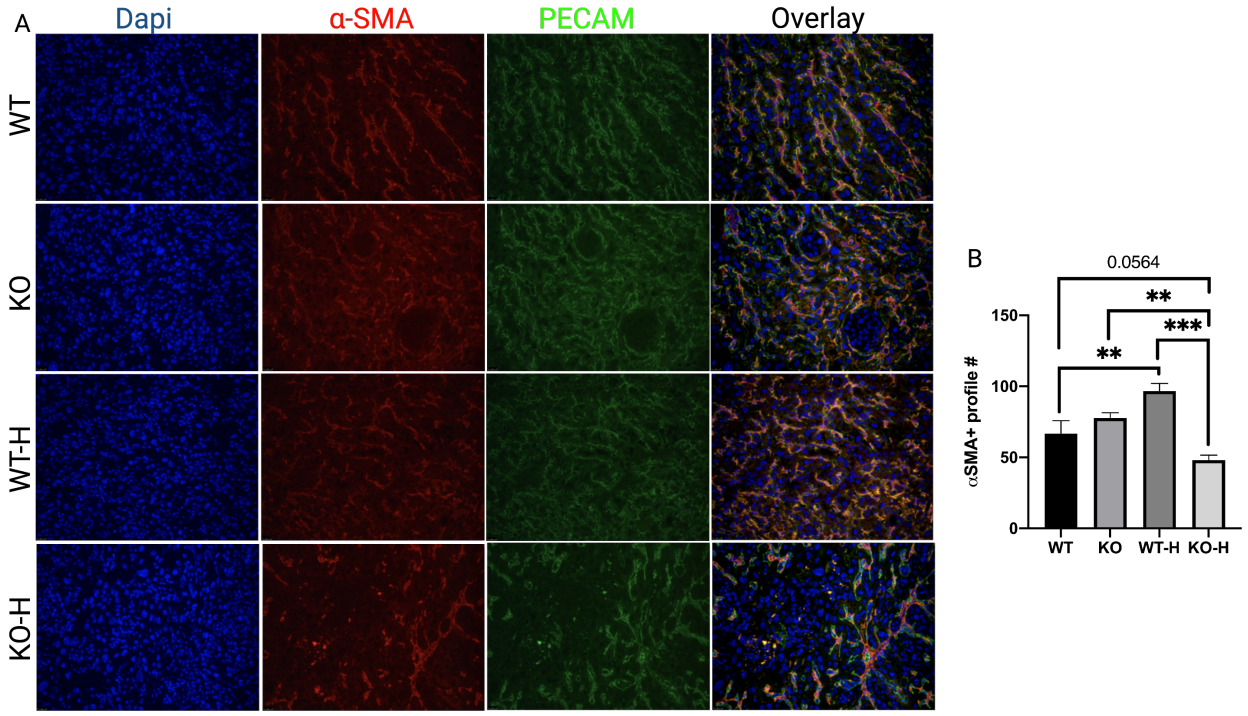

Figure 22. PCSK6 KO-H has the least amount of pericyte development due to the influence of *PCSK6 KO* and hyperglycemia. (A) Co-IF of α-SMA and PECAM in the Lab. (B) Number of α-SMA+ profiles in the Lab. Profiles refer to any α-SMA+ particles regardless of size. Fisher LSD's p-values are noted as *($p<0.05$), **($p<0.01$), ***($p<0.001$), ****($p<0.0001$). n=3 from m=3 per group. Created with BioRender.com.

Table 19. Two-way ANOVA results for αSMA+ profiles. Results of the test are reported as p-values noted as ns ($p>0.1$), *($p<0.05$), **($p<0.01$), ***($p<0.001$), ****($p<0.0001$).

2-way ANOVA	**αSMA profile**
Hyperglycemia effect	ns
***PCSK6 KO* effect**	*
Interaction	**

CHAPTER IV

SUMMARY AND DISCUSSION

Hyperglycemia is known to interrupt the placenta development.[87] We and others have found that placental PCSK6 levels decreased under hyperglycemia.[19] To address the important role of PCSK6 and to understand how it interacts with hyperglycemia in placenta development, phenotypes of *PCSK6 WT* and *KO* placentas involving GlyT differentiation, SpA remodeling, and angiogenesis in normoglycemic and hyperglycemic pregnancies were evaluated. The interaction between the environment factor—hyperglycemia, and the *PCSK6* gene on placenta development were assessed by two-way ANOVA and simple linear regression. In our study, *PCSK6 KO* decreased embryo weight, and its interaction with hyperglycemia decreased placenta weight. Hyperglycemia, but not *PCSK6 KO* or their interaction, increased the area of GlyTs within the Jz by increasing differentiation into the GlyT cell type. Overall, *PCSK6 KO* itself hindered SpA remodeling independent of hyperglycemia, evidenced by decreased LD, SpA LD/OD ratio, and SpA-TGC association. *PCSK6 KO* also induced a glucose dependent angiogenic response, contributing to increased diffusion capacity under normal glucose but decreased diffusion capacity under hyperglycemia.

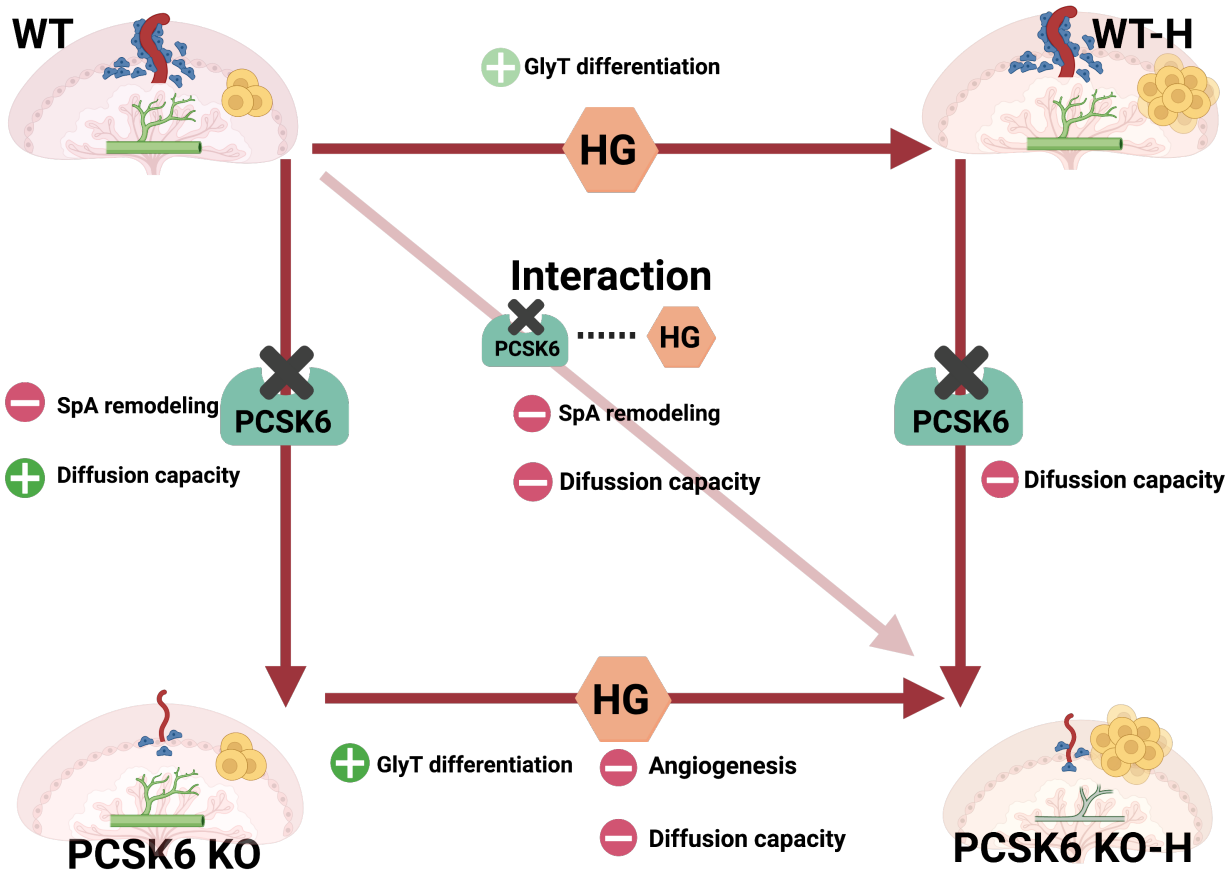

Figure 23. Summary of results. Each trend of dependent variables indicated by plus or minus signs are from the Fisher LSD test or $\chi 2$ test. The listed trends under interaction are from Fisher LSD results or $\chi 2$ test that compared WT and KO-H. Created with BioRender.com.

In our study, STZ treatment successfully induced hyperglycemia after pregnancy, which mimicked GDM conditions. Robust hyperglycemia was confirmed at E7.5, which allows us to investigate the effect of hyperglycemia on SpA remodeling which happens around E7.5~E10.5.[21] GlyTs undergo a lytic phase around E17.5 to form large glycogen lacunae near vascular sinuses.[88] This structure suggests that GlyTs supply energy towards the end of term.[88,89] Research is needed to understand the temporal and special role of GlyT in normal and gestational diseases. GlyT in gestational diseases is very difficult to study with human placenta due to the dynamic nature of GlyT content throughout the course of pregnancies.[90] Therefore, mouse models such as ours allow for evaluation of GlyT function during placenta development instead

of human term placentas that have already undergone development. From the PAS and Tpbpα+ staining, we reported that hyperglycemia, but not *PCSK6 KO*, increases the GlyT cell area within the Jz by increased differentiation. These changes in cell type distribution in the Jz could potentially impact the growth of the placenta and embryo. The majority of genetic mouse models found reduced glycogen content and/or GlyT phenotypes to be associated with fetal growth restriction, although some found the opposite relationship.[90] Interestingly, increased glycogen stores in the placenta have been observed in preeclampsia and GDM.[91,92] The presence of aberrant GlyT phenotypes suggests GlyT to be involved in the etiology of both GDM and preeclampsia. Given the hypothesized role of GlyT regulating growth hormones, such as insulin-like growth factor 2 (IGF2), and supply of energy,[90,93-95] careful attention to GlyT's role in mediating glucose dependent angiogenesis and growth factor transcription could lead to more information on GlyT function in the etiology of gestational diseases.

Defective SpA remodeling is implicated in early-onset preeclampsia and fetal growth restriction.[51] Normally, SpA remodeling by uNKs and EVT invasion ultimately makes the SpA vessel wall thinner and widens the lumen.[30] The *PCSK6 KO* groups had issues with the remodeling of the SpA arterial wall, resulting in smaller LD and smaller LD to OD ratios that indicate SpAs to be highly-resistant and low blood flow, characteristics seen in pathological pregnancies.[28] In our study, we further reported that *PCSK6 KO* hindered TGC association with SpAs. Issues with migration of trophoblasts have been described in abnormal SpA remodeling, as well as preeclampsia.[96] Future cell studies with HTR-8/SVneo using *PCSK6* siRNA, high glucose medium, and their combination will provide insight into the role of PCSK6 on expression of migratory genes and proteins on a cellular level. Additionally, wound healing and trans-well assays can be performed to investigate the effect of *PCSK6 KO*, hyperglycemia, and

their interaction on the ability of these cells to migrate and invade, respectively. As our model showed, *PCSK6 KO* significantly hindered SpA remodeling, which suggests PCSK6 to play a role in that process. Our results are exciting as further investigation of how *PCSK6 KO* led to hindered SpA remodeling could potentially shed light to future prevention strategies of pregnancy induced hypertension and preeclampsia.

The canonical Wnt signaling has been described to be involved in trophoblast migration.[37] In this pathway, free, non-phosphorylated β-catenin translocate into the nucleus to increase the transcription of migratory proteins.[37,38,40,41] When phosphorylated by GSK3β, β-catenin is marked for degradation and is unable to promote migration.[37,38] In our study, PCSK6 deletion significantly increased the phosphorylation of β-catenin, suggesting that there could be a decrease in transcription of migratory genes such as MMP-9 and MT1-MMP which have been independantly associated with the placenta and migratory cells.[40,42,43] Changes in these gene expressions will need to be investigated with qPCR. We also plan to investigate changes in GSK3β levels, GSK3β phosphorylation, Wnt ligands, and AKT phosphorylation which will allow for a fuller picture of how PCSK6 could be involved in regulating migratory factors.

TGFβ1 levels were found to be elevated in the plasma of preeclamptic women.[36] Although some discrepancies exist, TGFβ1 has mostly been described to inhibit cell migration.[32-35] The difference observed in these cell studies could be due to the differences in SMAD7 levels caused by performing the experiments on cells grown for different passages.[35] In our study, mature and latent TGFβ1 levels in Jz+Db lysates were decreased by hyperglycemia. Mature TGFβ1 levels were also decreased by *PCSK6 KO* in Jz+Db lysates. From the observation of reduced SpA remodeling in *PCSK6 KO* groups, the reduction of TGFβ1 in E14.5 *PCSK6 KO* placentas could be a compensatory mechanism to reduce the inhibitory effect of TGFβ1 on

migration, in turn promoting TGC migration. Future studies will need to test this hypothesis. Another possible explanation of how these altered TGFβ1 levels could affect placenta development is angiogenesis. TGFβ1 signaling has been described to be crucial for normal angiogenesis and vessel maturation in the Lab.[97-99] In the human placenta, TGFβ1 is expressed in the cytoplasm of both SynTs and cytotrophoblasts.[100] However, given that TGFβ1 is a secretory protein,[101] the levels of TGFβ1 protein detected in the Jz+Db lysate could have a role in Lab angiogenesis. Given the role of TGFβ1 in angiogenesis, a closer look into the molecular pathways regarding TGFβ1 signaling in the Lab affected by *PCSK6 KO*, hyperglycemia, and its interaction is warranted.

Issues with the SpA VSMC breakdown, normally aided by uNKs, could also contribute to abnormal SpA remodeling.[30] From the human protein atlas data, PCSK6 was reported to be high in NKs.[16] In our current analysis, we investigated the effect of global PCSK6 KO in both the placenta and maternal tissue. To further clarify if the changes we observed are due to placental PCSK6 KO or maternal KO, additional experiments will be needed. Considering that placenta is an organ composed of a mixture of cells derived from both mother and the fetus, and uNK cells are of maternal origin, comparison of SpA remodeling between placentas of *PCSK6*+/- embryos conceived by *PCSK6 WT* mothers and *PCSK6*+/- embryos conceived by *PCSK6 KO* mothers may provide more insight whether the observed issues with SpA remodeling is caused by a dysfunctional PCSK6 in uNK. Additionally, qPCR analysis of uNK cytokines in the Jz+Db layer in earlier stages of development, such as E7.5 to E10.5 may be performed.

Poor placenta angiogenesis can lead to fetal growth restriction.[102] In our study, *PCSK6 KO* under NG had increased diffusion capacity while the opposite was observed under HG. Early in the pregnancy, hypoxia stimulates the expression of angiogenic factors such as VEGF to

promote endothelial cell proliferation.[103] In our study, the FCA, regardless of significance, had the same trend as the VEGFA levels. FCA and VEGFA levels in KO placentas were slightly increased but statistically not different from WT levels while KO-H placentas had decreased levels (not significant) of FBS and VEGFA (marginally significant) compared to WT placentas. Additionally, the IHM thickness was significantly increased in the KO-H placentas whereas KO placentas did not see such change. With these factors combined, the diffusion capacity shows a clear angiogenic response in *PCSK6 KO* groups that is glucose dependent. Considering the issues in SpA remodeling caused by deletion of PCSK6, it appears that under NG, there is a compensatory angiogenic response, perhaps stimulated by hypoxia evidenced by normal VEGFA levels. Hypervascularity, often observed in GDM, has been attributed to decreased VEGFR1 and increased VEGFR2 expression.[50] Indeed, VEGFR1 and VEGFR2 mRNA levels were decreased and increased, respectively, in our hyperglycemic groups. The opposite angiogenic phenotype of *PCSK6 KO* placentas under hyperglycemia suggests that the angiogenic response to *PCSK6 KO*-induced hypoxia caused by poor SpA remodeling did not suffice to promote angiogenesis, and rather hindered angiogenesis under the combined influenced with hyperglycemia.

In humans, diabetic pregnancies result in early growth retardation in the first trimester (14 weeks).[104] However, diabetic pregnancies also have increased risk of macrosomia due to fetal growth acceleration that starts in the second trimester (18 weeks).[105] In our study, samples were collected at E14.5 which is equivalent to week 14 or the beginning of 2nd trimester.[31] At E14.5, embryo weight was decreased by hyperglycemia and *PCSK6 KO*. This decrease in embryo weight seen among hyperglycemic groups is consistent with the early growth retardation observed in early human diabetic pregnancies.[104] We are the first to report on the early growth restriction to be caused by *PCSK6 KO*. Additional sample collection at later stages of gestation is

needed to evaluate how the growth pattern changes over time, as catch-up growth has been observed among human diabetic pregnancies.[105] In addition, Lab nutrient transporters for amino acids, glucose, and fatty acids will also be detected with qPCR to further supplement the understanding for placental and embryonic growth. Among the embryos collected, the *PCSK6 KO* groups had several neural tube and craniofacial defects. This result is consistent with a previous study that also found craniofacial defects in *PCSK6 KO* embryos.[17] The same study also found that *PCSK6 KO* embryos had increased rates of DORV,[17] which was not observed to a significant level in our study possibly due to small sample size. Consistent with previous reports that hyperglycemia increases risks of cardiac defects[106], we observed more DORV in WT embryos under hyperglycemia. Notably, significantly higher incidence of neural tube defects, craniofacial defects and OFT defects were found in the KO-H embryos, suggesting a synergic effect of PCSK6 deletion and hyperglycemia on birth defects.

Limitations of this study is that we utilized a germline *PCSK6 KO* mouse line which does not allow us to pinpoint the cause of the observed phenotypes to the placental *PCSK6 KO* or maternal *PCSK6 KO*. Specifically, one of the possible maternal symptoms that could affect placenta development is hypertension caused by maternal *PCSK6 KO*. As *PCSK6 KO* has been reported to cause salt-sensitive hypertension, maternal *PCSK6 KO* itself may cause hypertension before and/or upon pregnancy.[72] Clarification of the baseline and changes in clinical metrics of preeclampsia such as blood pressure and urine protein will provide insight if the clinical features are due to *PCSK6 KO* regardless of pregnancy or pregnancy-induced. From our data, PCSK6 was found to be specifically expressed in the GlyT of the Jz. Assessing placentas from crossing a *PCSK6-Flox* with *Tpbpα-cre* mouse would allow us to investigate the role of PCSK6 specifically in the Jz, and ultimately its role in placenta development independent of maternal PCSK6.

Further investigation is needed to answer which specific substrates of PCSK6 affect SpA remodeling and glucose-dependent angiogenesis. It is worth noting that most previous reports on PCSK6 action was reported to be in the ECM. However, some suggest that PCSK6 can also temporality access intracellular substrates during transport because PCSK6 is secreted into the ECM in a constitutive pathway.[60,107] Therefore, it is important to not limit potential PCSK6 substrates to extracellular proteins. Candidates for PCSK6 substrates will be identified from mass-spectrometry based proteomics. When new potential candidates for PCSK6 are identified, WB for expression change, immunoprecipitation for interaction, and peptide cleavage assay for protease activity will be performed. Future experiments using HTR-8/SVneo cell line to detect changes in levels of candidate proteins and cell migration/invasion upon target gene siRNA treatment, and phenotypes of transgenic mice with mutation in the candidate protein will be used to study their functional role in placenta development.

To our knowledge, this study is the first to investigate the role of PCSK6 on the placenta development *in vivo*. Literature on GlyT function in placenta development and gestational diseases is scarce which makes the expression of PCSK6 in GlyT, and its role in SpA remodeling, and glucose dependent angiogenesis a novel discovery. Our study will elucidate the role of PCSK6 in these processes which will contribute to the understanding of preeclampsia and GDM pathogenesis and their etiology.

REFERENCES

1. Heindel JJ, Vandenberg LN. Developmental origins of health and disease: a paradigm for understanding disease cause and prevention. *Curr Opin Pediatr.* 2015;27(2):248-253.

2. Wadhwa PD, Buss C, Entringer S, Swanson JM. Developmental origins of health and disease: brief history of the approach and current focus on epigenetic mechanisms. *Semin Reprod Med.* 2009;27(5):358-368.

3. National Institute of Health. Human Placenta Project. https://www.nichd.nih.gov/research/supported/HPP/default. Published 2020. Accessed March 22, 2021.

4. Flegal KM, Carroll MD, Kit BK, Ogden CL. Prevalence of obesity and trends in the distribution of body mass index among US adults, 1999-2010. *Jama.* 2012;307(5):491-497.

5. Lin PC, Hung CH, Chan TF, Lin KC, Hsu YY, Ya-Ling T. The risk factors for gestational diabetes mellitus: A retrospective study. *Midwifery.* 2016;42:16-20.

6. Bartsch E, Medcalf KE, Park AL, Ray JG. Clinical risk factors for pre-eclampsia determined in early pregnancy: systematic review and meta-analysis of large cohort studies. *BMJ.* 2016;353:i1753.

7. Casagrande SS, Linder B, Cowie CC. Prevalence of gestational diabetes and subsequent Type 2 diabetes among U.S. women. *Diabetes Res Clin Pract.* 2018;141:200-208.

8. Ananth CV, Keyes KM, Wapner RJ. Pre-eclampsia rates in the United States, 1980-2010: age-period-cohort analysis. *BMJ : British Medical Journal.* 2013;347:f6564.

9. Innes KE, Wimsatt JH. Pregnancy-induced hypertension and insulin resistance: evidence for a connection. *Acta Obstet Gynecol Scand.* 1999;78(4):263-284.

10. Suhonen L, Teramo K. Hypertension and pre-eclampsia in women with gestational glucose intolerance. *Acta Obstetricia et Gynecologica Scandinavica.* 1993;72(4):269-272.

11. Garner PR, D'Alton ME, Dudley DK, Huard P, Hardie M. Preeclampsia in diabetic pregnancies. *Am J Obstet Gynecol.* 1990;163(2):505-508.

12. Lee J, Ouh Y-T, Ahn KH, et al. Preeclampsia: A risk factor for gestational diabetes mellitus in subsequent pregnancy. *PloS one.* 2017;12(5):e0178150-e0178150.

13. Ilekis JV, Tsilou E, Fisher S, et al. Placental origins of adverse pregnancy outcomes: potential molecular targets: an Executive Workshop Summary of the Eunice Kennedy

Shriver National Institute of Child Health and Human Development. *American Journal of Obstetrics and Gynecology.* 2016;215(1, Supplement):S1-S46.

14. Sucic JF, Moehring JM, Inocencio NM, Luchini JW, Moehring TJ. Endoprotease PACE4 is Ca2+-dependent and temperature-sensitive and can partly rescue the phenotype of a furin-deficient cell strain. *Biochem J.* 1999;339 (Pt 3)(Pt 3):639-647.

15. Seidah NG, Chrétien M. Proprotein and prohormone convertases: a family of subtilases generating diverse bioactive polypeptides. *Brain Research.* 1999;848(1):45-62.

16. Uhlén M, Fagerberg L, Hallström BM, et al. Tissue-based map of the human proteome. *Science.* 2015;347(6220):1260419.http://www.proteinatlas.org. Image credit: Human Protein Atlas. Image/gene/data available from v20.proteinatlas.org/ENSG00000140479-PCSK00000140476/tissue, v20.proteinatlas.org/ENSG00000140479-PCSK00000140476/celltype, and v20.proteinatlas.org/ENSG00000140479-PCSK00000140476/blood.

17. Constam DB, Robertson EJ. SPC4/PACE4 regulates a TGFbeta signaling network during axis formation. *Genes & development.* 2000;14(9):1146-1155.

18. Rykaczewska U, Suur BE, Rohl S, et al. PCSK6 Is a Key Protease in the Control of Smooth Muscle Cell Function in Vascular Remodeling. *Circulation research.* 2020;126(5):571-585.

19. Abassi Z, Kinaneh S, Skarzinski G, et al. Aberrant corin and PCSK6 in placentas of the maternal hyperinsulinemia IUGR rat model. *Pregnancy Hypertension.* 2020;21:70-76.

20. Barreto RSN, Romagnolli P, Cereta AD, Coimbra-Campos LMC, Birbrair A, Miglino MA. Pericytes in the Placenta: Role in Placental Development and Homeostasis. *Adv Exp Med Biol.* 2019;1122:125-151.

21. Woods L, Perez-Garcia V, Hemberger M. Regulation of Placental Development and Its Impact on Fetal Growth—New Insights From Mouse Models. *Frontiers in Endocrinology.* 2018;9(570).

22. Georgiades P, Ferguson-Smith AC, Burton GJ. Comparative Developmental Anatomy of the Murine and Human Definitive Placentae. *Placenta.* 2002;23(1):3-19.

23. Moreau JLM, Artap ST, Shi H, et al. Cited2 is required in trophoblasts for correct placental capillary patterning. *Developmental Biology.* 2014;392(1):62-79.

24. Coan PM, Ferguson-Smith AC, Burton GJ. Developmental Dynamics of the Definitive Mouse Placenta Assessed by Stereology. *Biology of Reproduction.* 2004;70(6):1806-1813.

25. Mori M, Bogdan A, Balassa T, Csabai T, Szekeres-Bartho J. The decidua—the maternal bed embracing the embryo—maintains the pregnancy. *Seminars in Immunopathology.* 2016;38(6):635-649.

26. Simmons DG, Fortier AL, Cross JC. Diverse subtypes and developmental origins of trophoblast giant cells in the mouse placenta. *Developmental Biology.* 2007;304(2):567-578.

27. Soncin F, Natale D, Parast MM. Signaling pathways in mouse and human trophoblast differentiation: a comparative review. *Cell Mol Life Sci.* 2015;72(7):1291-1302.

28. Burton GJ, Woods AW, Jauniaux E, Kingdom JC. Rheological and physiological consequences of conversion of the maternal spiral arteries for uteroplacental blood flow during human pregnancy. *Placenta.* 2009;30(6):473-482.

29. Whitley GSJ, Cartwright JE. Cellular and molecular regulation of spiral artery remodelling: lessons from the cardiovascular field. *Placenta.* 2010;31(6):465-474.

30. Cartwright J, Fraser R, Leslie K, Wallace A, James J. Remodelling at the maternal-fetal interface: Relevance to human pregnancy disorders. *Reproduction (Cambridge, England).* 2010;140:803-813.

31. Ander SE, Diamond MS, Coyne CB. Immune responses at the maternal-fetal interface. *Science Immunology.* 2019;4(31):eaat6114.

32. Huang Z, Li S, Fan W, Ma Q. Transforming growth factor β1 promotes invasion of human JEG-3 trophoblast cells via TGF-β/Smad3 signaling pathway. *Oncotarget.* 2017;8(20):33560-33570.

33. Cheng JC, Chang HM, Leung PC. Transforming growth factor-β1 inhibits trophoblast cell invasion by inducing Snail-mediated down-regulation of vascular endothelial-cadherin protein. *J Biol Chem.* 2013;288(46):33181-33192.

34. Lash GE, Otun HA, Innes BA, Bulmer JN, Searle RF, Robson SC. Inhibition of trophoblast cell invasion by TGFB1, 2, and 3 is associated with a decrease in active proteases. *Biol Reprod.* 2005;73(2):374-381.

35. Zuo Y, Fu Z, Hu Y, et al. Effects of transforming growth factor-β1 on the proliferation and invasion of the HTR-8/SVneo cell line. *Oncol Lett.* 2014;8(5):2187-2192.

36. Peraçoli MT, Menegon FT, Borges VT, de Araújo Costa RA, Thomazini-Santos IA, Peraçoli JC. Platelet aggregation and TGF-beta(1) plasma levels in pregnant women with preeclampsia. *J Reprod Immunol.* 2008;79(1):79-84.

37. Knöfler M, Pollheimer J. Human placental trophoblast invasion and differentiation: a particular focus on Wnt signaling. *Front Genet.* 2013;4:190-190.

38. Thompson M, Nejak-Bowen K, Monga SPS. Crosstalk of the Wnt Signaling Pathway. In: Goss KH, Kahn M, eds. *Targeting the Wnt Pathway in Cancer.* New York, NY: Springer New York; 2011:51-80.

39. Metcalfe C, Bienz M. Inhibition of GSK3 by Wnt signalling – two contrasting models. *Journal of Cell Science.* 2011;124(21):3537.

40. Ingraham CA, Park GC, Makarenkova HP, Crossin KL. Matrix Metalloproteinase (MMP)-9 Induced by Wnt Signaling Increases the Proliferation and Migration of Embryonic Neural Stem Cells at Low O2 Levels. *Journal of Biological Chemistry.* 2011;286(20):17649-17657.

41. Takahashi M, Tsunoda T, Seiki M, Nakamura Y, Furukawa Y. Identification of membrane-type matrix metalloproteinase-1 as a target of the beta-catenin/Tcf4 complex in human colorectal cancers. *Oncogene.* 2002;21(38):5861-5867.

42. Bjørn SF, Hastrup N, Lund LR, Danø K, Larsen JF, Pyke C. Co-ordinated expression of MMP-2 and its putative activator, MT1-MMP, in human placentation. *Mol Hum Reprod.* 1997;3(8):713-723.

43. Zhang Y, Li P, Guo Y, Liu X, Zhang Y. MMP-9 and TIMP-1 in placenta of hypertensive disorder complicating pregnancy. *Exp Ther Med.* 2019;18(1):637-641.

44. Chen D-B, Zheng J. Regulation of placental angiogenesis. *Microcirculation.* 2014;21(1):15-25.

45. Ohlsson R, Falck P, Hellström M, et al. PDGFB regulates the development of the labyrinthine layer of the mouse fetal placenta. *Dev Biol.* 1999;212(1):124-136.

46. Plows JF, Stanley JL, Baker PN, Reynolds CM, Vickers MH. The Pathophysiology of Gestational Diabetes Mellitus. *International journal of molecular sciences.* 2018;19(11):3342.

47. Jarmuzek P, Wielgos M, Bomba-Opon D. Placental pathologic changes in gestational diabetes mellitus. *Neuro Endocrinol Lett.* 2015;36(2):101-105.

48. Stanek J. Hypoxic Patterns of Placental Injury: A Review. *Archives of Pathology & Laboratory Medicine.* 2013;137(5):706-720.

49. Kadyrov N, Kosanke G, Kingdom J, Kaufmann P. Increased fetoplacental angiogenesis during first trimester in anaemic women. *The Lancet.* 1998;352(9142):1747-1749.

50. Troncoso F, Acurio J, Herlitz K, et al. Gestational diabetes mellitus is associated with increased pro-migratory activation of vascular endothelial growth factor receptor 2 and reduced expression of vascular endothelial growth factor receptor 1. *PloS one.* 2017;12(8):e0182509-e0182509.

51. Albrecht ED, Pepe GJ. Regulation of Uterine Spiral Artery Remodeling: a Review. *Reproductive Sciences.* 2020;27(10):1932-1942.

52. Staff AC. The two-stage placental model of preeclampsia: An update. *J Reprod Immunol.* 2019;134-135:1-10.

53. Lopez-Jaramillo P, Barajas J, Rueda-Quijano SM, Lopez-Lopez C, Felix C. Obesity and Preeclampsia: Common Pathophysiological Mechanisms. *Frontiers in Physiology.* 2018;9(1838).

54. Jeyabalan A. Epidemiology of preeclampsia: impact of obesity. *Nutrition reviews.* 2013;71 Suppl 1(0 1):S18-S25.

55. Bryson CL, Ioannou GN, Rulyak SJ, Critchlow C. Association between Gestational Diabetes and Pregnancy-induced Hypertension. *American Journal of Epidemiology.* 2003;158(12):1148-1153.

56. Levine RJ, Maynard SE, Qian C, et al. Circulating angiogenic factors and the risk of preeclampsia. *N Engl J Med.* 2004;350(7):672-683.

57. El-Tarhouny SA, Almasry SM, Elfayomy AK, Baghdadi H, Habib FA. Placental growth factor and soluble Fms-like tyrosine kinase 1 in diabetic pregnancy: A possible relation to distal villous immaturity. *Histol Histopathol.* 2014;29(2):259-272.

58. Hauth JC, Clifton RG, Roberts JM, et al. Maternal insulin resistance and preeclampsia. *American journal of obstetrics and gynecology.* 2011;204(4):327.e321-327.e3276.

59. Seidah NG, Chrétien M. Proprotein and prohormone convertases: a family of subtilases generating diverse bioactive polypeptides. *Brain Res.* 1999;848(1-2):45-62.

60. Nagahama M, Taniguchi T, Hashimoto E, et al. Biosynthetic processing and quaternary interactions of proprotein convertase SPC4 (PACE4). *FEBS Letters.* 1998;434(1):155-159.

61. Tsuji A, Sakurai K, Kiyokage E, et al. Secretory proprotein convertases PACE4 and PC6A are heparin-binding proteins which are localized in the extracellular matrix. Potential role of PACE4 in the activation of proproteins in the extracellular matrix. *Biochim Biophys Acta.* 2003;1645(1):95-104.

62. Merton Bernfield, Martin Götte, Pyong Woo Park, et al. Functions of Cell Surface Heparan Sulfate Proteoglycans. *Annual Review of Biochemistry.* 1999;68(1):729-777.

63. Paine-Saunders S, Viviano BL, Zupicich J, Skarnes WC, Saunders S. glypican-3 Controls Cellular Responses to Bmp4 in Limb Patterning and Skeletal Development. *Developmental Biology.* 2000;225(1):179-187.

64. Soulintzi N, Zagris N. Spatial and temporal expression of perlecan in the early chick embryo. *Cells Tissues Organs.* 2007;186(4):243-256.

65. Wallon UM, Overall CM. The Hemopexin-like Domain (C Domain) of Human Gelatinase A (Matrix Metalloproteinase-2) Requires Ca2+ for Fibronectin and Heparin Binding: BINDING PROPERTIES OF RECOMBINANT GELATINASE A C DOMAIN TO EXTRACELLULAR MATRIX AND BASEMENT MEMBRANE COMPONENTS*. *Journal of Biological Chemistry.* 1997;272(11):7473-7481.

66. Wang P, Wang F, Wang L, Pan J. Proprotein convertase subtilisin/kexin type 6 activates the extracellular signal-regulated kinase 1/2 and Wnt family member 3A pathways and promotes in vitro proliferation, migration and invasion of breast cancer MDA-MB-231 cells. *Oncol Lett.* 2018;16(1):145-150.

67. D'Anjou F, Routhier S, Perreault JP, et al. Molecular Validation of PACE4 as a Target in Prostate Cancer. *Transl Oncol.* 2011;4(3):157-172.

68. Mahloogi H, Bassi DE, Klein-Szanto AJP. Malignant conversion of non-tumorigenic murine skin keratinocytes overexpressing PACE4. *Carcinogenesis.* 2002;23(4):565-572.

69. Constam DB, Robertson EJ. Regulation of bone morphogenetic protein activity by pro domains and proprotein convertases. *J Cell Biol.* 1999;144(1):139-149.

70. Wang Y, Wang XH, Fan DX, et al. PCSK6 regulated by LH inhibits the apoptosis of human granulosa cells via activin A and TGFβ2. *J Endocrinol.* 2014;222(1):151-160.

71. Mujoomdar M, Hogan L, Parlow A, Nachtigal M. Pcsk6 mutant mice exhibit progressive loss of ovarian function, altered gene expression, and formation of ovarian pathology. *Reproduction (Cambridge, England).* 2011;141:343-355.

72. Chen S, Cao P, Dong N, et al. PCSK6-mediated corin activation is essential for normal blood pressure. *Nature medicine.* 2015;21(9):1048-1053.

73. Cui Y, Wang W, Dong N, et al. Role of corin in trophoblast invasion and uterine spiral artery remodelling in pregnancy. *Nature.* 2012;484(7393):246-250.

74. Perisic L, Hedin E, Razuvaev A, et al. Profiling of atherosclerotic lesions by gene and tissue microarrays reveals PCSK6 as a novel protease in unstable carotid atherosclerosis. *Arterioscler Thromb Vasc Biol.* 2013;33(10):2432-2443.

75. Rykaczewska U, Suur Bianca E, Röhl S, et al. PCSK6 Is a Key Protease in the Control of Smooth Muscle Cell Function in Vascular Remodeling. *Circulation research.* 2020;126(5):571-585.

76. Itoh Y. Membrane-type matrix metalloproteinases: Their functions and regulations. *Matrix Biol.* 2015;44-46:207-223.

77. Sato H, Takino T, Okada Y, et al. A matrix metalloproteinase expressed on the surface of invasive tumour cells. *Nature.* 1994;370(6484):61-65.

78. Lehti K, Lohi J, Juntunen MM, Pei D, Keski-Oja J. Oligomerization through Hemopexin and Cytoplasmic Domains Regulates the Activity and Turnover of Membrane-type 1 Matrix Metalloproteinase *. *Journal of Biological Chemistry.* 2002;277(10):8440-8448.

79. Tsunezuka Y, Kinoh H, Takino T, et al. Expression of Membrane-type Matrix Metalloproteinase 1 (MT1-MMP) in Tumor Cells Enhances Pulmonary Metastasis in an Experimental Metastasis Assay. *Cancer Research.* 1996;56(24):5678-5683.

80. Hotary KB, Allen ED, Brooks PC, Datta NS, Long MW, Weiss SJ. Membrane Type I Matrix Metalloproteinase Usurps Tumor Growth Control Imposed by the Three-Dimensional Extracellular Matrix. *Cell.* 2003;114(1):33-45.

81. Hiraoka N, Allen E, Apel IJ, Gyetko MR, Weiss SJ. Matrix Metalloproteinases Regulate Neovascularization by Acting as Pericellular Fibrinolysins. *Cell.* 1998;95(3):365-377.

82. Choi S, Korstanje R. Proprotein convertases in high-density lipoprotein metabolism. *Biomark Res.* 2013;1(1):27-27.

83. Jin W, Fuki IV, Seidah NG, Benjannet S, Glick JM, Rader DJ. Proprotein Covertases Are Responsible for Proteolysis and Inactivation of Endothelial Lipase*. *Journal of Biological Chemistry.* 2005;280(44):36551-36559.

84. Szkudelski T. The mechanism of alloxan and streptozotocin action in B cells of the rat pancreas. *Physiol Res.* 2001;50(6):537-546.

85. Devisme L, Merlot B, Ego A, Houfflin-Debarge V, Deruelle P, Subtil D. A case–control study of placental lesions associated with pre-eclampsia. *International Journal of Gynecology & Obstetrics.* 2013;120(2):165-168.

86. Lacko LA, Hurtado R, Hinds S, Poulos MG, Butler JM, Stuhlmann H. Altered feto-placental vascularization, feto-placental malperfusion and fetal growth restriction in mice with Egfl7 loss of function. *Development (Cambridge, England).* 2017;144(13):2469-2479.

87. Nteeba J, Varberg KM, Scott RL, Simon ME, Iqbal K, Soares MJ. Poorly controlled diabetes mellitus alters placental structure, efficiency, and plasticity. *BMJ Open Diabetes Research & Care.* 2020;8(1):e001243.

88. Bouillot S, Rampon C, Tillet E, Huber P. Tracing the Glycogen Cells with Protocadherin 12 During Mouse Placenta Development. *Placenta.* 2006;27(8):882-888.

89. Akison LK, Nitert MD, Clifton VL, Moritz KM, Simmons DG. Review: Alterations in placental glycogen deposition in complicated pregnancies: Current preclinical and clinical evidence. *Placenta.* 2017;54:52-58.

90. Simon JT, Erica DW, Abigail LF, Graham JB. Placental glycogen stores and fetal growth: insights from genetic mouse models. *Reproduction.* 2020;159(6):R213-R235.

91. Arkwright PD, Rademacher TW, Dwek RA, Redman CW. Pre-eclampsia is associated with an increase in trophoblast glycogen content and glycogen synthase activity, similar to that found in hydatidiform moles. *J Clin Invest.* 1993;91(6):2744-2753.

92. Desoye G, Hofmann HH, Weiss PA. Insulin binding to trophoblast plasma membranes and placental glycogen content in well-controlled gestational diabetic women treated with diet or insulin, in well-controlled overt diabetic patients and in healthy control subjects. *Diabetologia.* 1992;35(1):45-55.

93. Kim J, Song G, Gao H, et al. Insulin-Like Growth Factor II Activates Phosphatidylinositol 3-Kinase-Protooncogenic Protein Kinase 1 and Mitogen-Activated Protein Kinase Cell Signaling Pathways, and Stimulates Migration of Ovine Trophectoderm Cells. *Endocrinology.* 2008;149(6):3085-3094.

94. White V, Jawerbaum A, Mazzucco MB, Gauster M, Desoye G, Hiden U. IGF2 stimulates fetal growth in a sex- and organ-dependent manner. *Pediatric Research.* 2018;83(1):183-189.

95. Coan PM, Conroy N, Burton GJ, Ferguson-Smith AC. Origin and characteristics of glycogen cells in the developing murine placenta. *Developmental Dynamics.* 2006;235(12):3280-3294.

96. Goldman-Wohl D, Yagel S. Regulation of trophoblast invasion: from normal implantation to pre-eclampsia. *Molecular and Cellular Endocrinology.* 2002;187(1):233-238.

97. Cerdeira AS, Karumanchi SA. Angiogenic factors in preeclampsia and related disorders. *Cold Spring Harb Perspect Med.* 2012;2(11):a006585.

98. Larsson J, Goumans MJ, Sjöstrand LJ, et al. Abnormal angiogenesis but intact hematopoietic potential in TGF-beta type I receptor-deficient mice. *The EMBO journal.* 2001;20(7):1663-1673.

99. Goumans MJ, Valdimarsdottir G, Itoh S, Rosendahl A, Sideras P, ten Dijke P. Balancing the activation state of the endothelium via two distinct TGF-beta type I receptors. *Embo j.* 2002;21(7):1743-1753.

100. Xuan YH, Choi YL, Shin YK, et al. Expression of TGF-beta signaling proteins in normal placenta and gestational trophoblastic disease. *Histol Histopathol.* 2007;22(3):227-234.

101. Xu X, Zheng L, Yuan Q, et al. Transforming growth factor-β in stem cells and tissue homeostasis. *Bone Research.* 2018;6(1):2.

102. Pereira RD, De Long NE, Wang RC, Yazdi FT, Holloway AC, Raha S. Angiogenesis in the Placenta: The Role of Reactive Oxygen Species Signaling. *BioMed Research International.* 2015;2015:814543.

103. Wang K, Jiang YZ, Chen DB, Zheng J. Hypoxia enhances FGF2- and VEGF-stimulated human placental artery endothelial cell proliferation: roles of MEK1/2/ERK1/2 and PI3K/AKT1 pathways. *Placenta.* 2009;30(12):1045-1051.

104. Pedersen JF, Mølsted-Pedersen L. Early growth retardation in diabetic pregnancy. *Br Med J.* 1979;1(6155):18-19.

105. Wong SF, Chan FY, Oats JJN, McIntyre DH. Fetal Growth Spurt and Pregestational Diabetic Pregnancy. *Diabetes Care.* 2002;25(10):1681.

106. Scott-Drechsel DE, Rugonyi S, Marks DL, Thornburg KL, Hinds MT. Hyperglycemia slows embryonic growth and suppresses cell cycle via cyclin D1 and p21. *Diabetes.* 2013;62(1):234-242.

107. Salvas A, Benjannet S, Reudelhuber TL, Chrétien M, Seidah NG. Evidence for proprotein convertase activity in the endoplasmic reticulum/early Golgi. *FEBS Letters.* 2005;579(25):5621-5625.